Quaternary Research 84 (2015) 368–381

Contents lists available at ScienceDirect

Quaternary Research

journal homepage: www.elsevier.com/locate/yqres

Reconstruction of a semi-arid late Pleistocene paleocatena from the Lake Victoria region, Kenya

Emily J. Beverly [a,*], Steven G. Driese [a], Daniel J. Peppe [a], L. Nicole Arellano [a], Nick Blegen [b], J. Tyler Faith [c], Christian A. Tryon [d]

[a] Terrestrial Paleoclimatology Research Group, Department of Geology, Baylor University, One Bear Place #97354, Waco, TX 76798-7354, USA
[b] Department of Anthropology, University of Connecticut, U-2176, Storrs, CT 06269, USA
[c] School of Social Science, University of Queensland, Brisbane, QLD 4072, Australia
[d] Department of Anthropology, Harvard University, Peabody Museum, 11 Divinity Ave., Cambridge, MA 02138, USA

ARTICLE INFO

Article history:
Received 2 April 2015
Available online 4 October 2015

Keywords:
Paleosols
Paleoenvironment
Karungu
Semi-arid
Paleoclimate
Human evolution

ABSTRACT

The effect of changing environment on the evolution of *Homo sapiens* is heavily debated, but few data are available from equatorial Africa prior to the last glacial maximum. The Karungu deposits on the northeast coast of Lake Victoria are ideal for paleoenvironmental reconstructions and are best studied at the Kisaaka site near Karunga in Kenya (94 to >33 ka) where paleosols, fluvial deposits, tufa, and volcaniclastic deposits (tuffs) are exposed over a ~2 km transect. Three well-exposed and laterally continuous paleosols with intercalated tuffs allow for reconstruction of a succession of paleocatenas. The oldest paleosol is a smectitic paleo-Vertisol with saline and sodic properties. Higher in the section, the paleosols are tuffaceous paleo-Inceptisols with Alfisol-like soil characteristics (illuviated clay). Mean annual precipitation (MAP) proxies indicate little change through time, with an average of 764 ± 108 mm yr^{-1} for Vertisols (CALMAG) and 813 ± 182 to 963 ± 182 mm yr^{-1} for all paleosols (CIA-K). Field observations and MAP proxies suggest that Karungu was significantly drier than today, consistent with the associated faunal assemblage, and likely resulted in a significantly smaller Lake Victoria during the late Pleistocene. Rainfall reduction and associated grassland expansion may have facilitated human and faunal dispersals across equatorial East Africa.

Introduction

Climate-driven environmental change is a commonly proposed mechanism for the dispersals of humans within and out of Africa through its effects on population distributions and demographics, biogeographic barriers, and resource availability (e.g., Ambrose and Lorenz, 1990; Scholz et al., 2007; Cowling et al., 2008; Blome et al., 2012; Eriksson et al., 2012; Soares et al., 2012; Rito et al., 2013; Faith et al., in press). The earliest fossil remains of *Homo sapiens* are known from East Africa at ~195 ka, and by as early as 80 to 60 ka populations had dispersed throughout Africa and also into Eurasia (e.g., McDougall et al., 2005; Brown et al., 2012; Soares et al., 2012; Rito et al., 2013). Few empirical data on climate or environment at relevant spatial or temporal scales are associated with archeological or early human fossil sites from equatorial East Africa prior to the last glacial maximum (LGM) (e.g., Blome et al., 2012), which limits understanding the ecology of early human populations and the mechanisms underlying their dispersals. Sediment cores from Lake Victoria provide continuous records of regional hydrology and vegetation back to the LGM (Kendall, 1969; Johnson et al., 1996; Talbot and Laerdal, 2000; Stager et al., 2002, 2011; Berke et al., 2012), but paleoenvironmental data prior to the LGM are sparse.

Deposits identified along the northeastern shores of Lake Victoria near Karungu, Kenya, dated to between 94 ka and >33 ka (Tryon et al., 2010; Beverly et al., 2015; Blegen et al., 2015; Faith et al., 2015), have the potential to provide fundamental paleoenvironmental and paleoclimatic information about equatorial East Africa during this critical interval of human evolution and dispersal (Fig. 1A and B). The sediments at Karungu preserve abundant vertebrate fossils and Middle Stone Age (MSA) artifacts (Owen, 1937; Pickford, 1984; Faith et al., 2015), which are considered the archeological signature of early *H. sapiens* in East Africa (McBrearty and Brooks, 2000; Tryon and Faith, 2013). The pre-LGM Karungu dataset complements, refines, and expands those from correlative deposits on Rusinga and Mfangano Islands ~40 km to the north (Tryon et al., 2010; Faith et al., 2011; Van Plantinga, 2011; Faith et al., 2012; Tryon et al., 2012; Faith et al., 2014; Tryon et al., 2014; Faith et al., 2015; Garrett et al., 2015). Previous evidence from MSA archeological and paleontological sites from Rusinga and Mfangano Islands suggests that the contraction of Lake Victoria and expansion of grasslands during the late Pleistocene may have facilitated the dispersal of large-bodied mammals, including humans, across Africa (e.g., Faith

* Corresponding author.
E-mail address: Emily_Beverly@Baylor.edu (E.J. Beverly).

http://dx.doi.org/10.1016/j.yqres.2015.08.002
0033-5894/

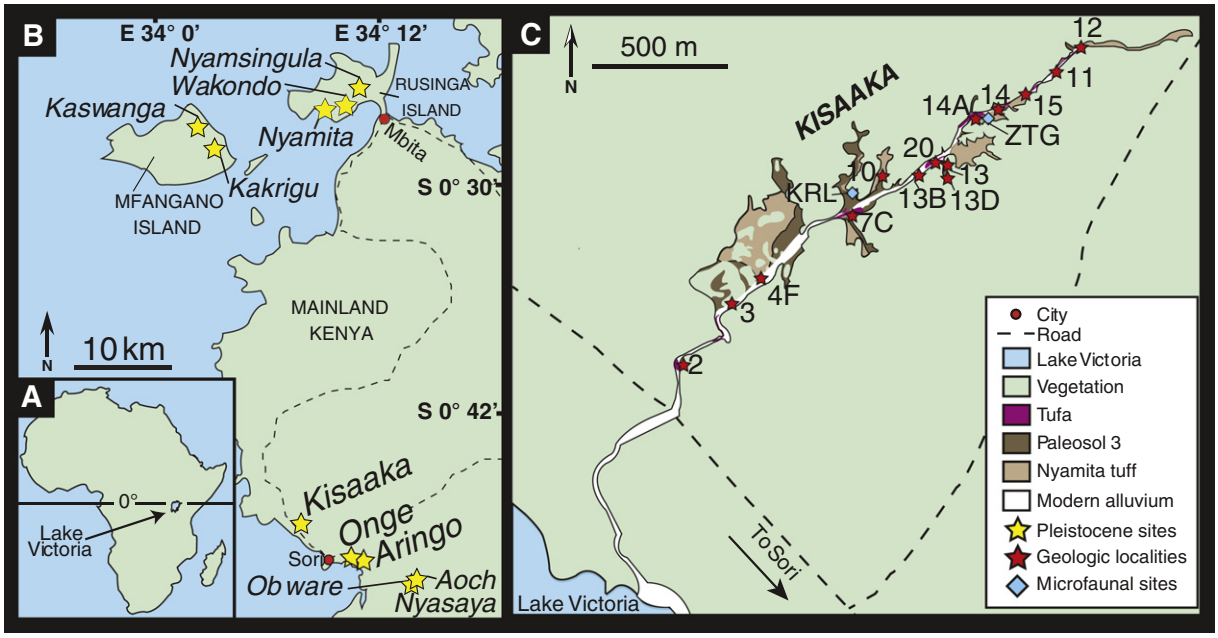

Figure 1. Location maps. A) Inset shows the location of Lake Victoria in East Africa. B) Location of Pleistocene sites along the eastern margin of Lake Victoria. C) Mapped lithologies exposed at the Kisaaka site with key geologic and microfaunal locations identified. Modified from Beverly et al. (2015).

et al., 2015, in press). However, the modeled reduction in the size of Lake Victoria requires a reduction in late-Pleistocene precipitation (Broecker et al., 1998; Milly, 1999), for which we had no direct evidence. Here, we provide the first quantitative estimates of paleoprecipitation through a multi-proxy analysis of paleosols from Kisaaka (Fig. 1C), one of seven Pleistocene artifact- and fossil-bearing

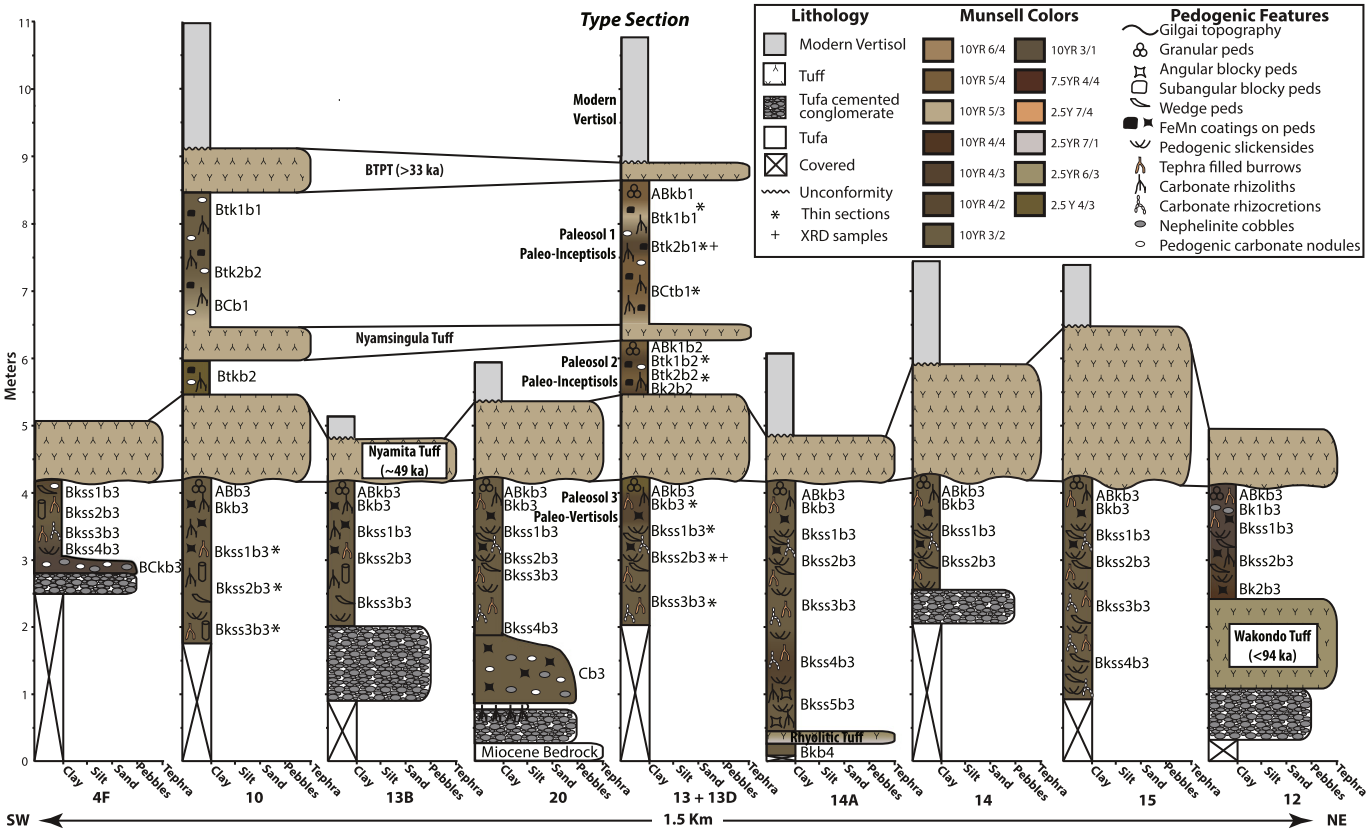

Figure 2. Measured stratigraphic sections from Kisaaka correlated using the base of the laterally extensive Nyamita Tuff as the datum and tephrostratigraphy by Blegen et al. (2015). Localities are arranged from north to south over 1.5 km transect. See Fig. 1 for location of sites. Pedogenic features, soil and tuff colors, soil horizons, and lithology are described in detail with three paleosols identified.

https://doi.org/10.1016/j.yqres.2015.08.002 Published online by Cambridge University Press

sites at Karungu, originally noted by Owen (1937, 1938, 1939), later mapped by Pickford (1984) and the focus of fieldwork by our team over the last several years (Faith et al., 2015).

The deposits at Kisaaka are predominantly made up of paleosols, which provide invaluable records of paleoenvironmental information through the use of paleosol paleoclimate proxies (reviewed in Sheldon and Tabor, 2009; Tabor and Myers, 2015). In addition, correlative tuffs blanketing the landscape allow for lithostratigraphic correlation between outcrops and in some instances the preservation of the original topography (Figs. 1C, 2, and 3A; Faith et al., 2015; Blegen et al., 2015). Milne (1936) originally defined the relationship of soil development to changes in topography as a catena, and soil properties can change dramatically across a landscape with topography due to changes in hydrology (Birkeland, 1999). The correlative volcanic ashes burying these surfaces form a succession of paleocatenas at Kisaaka. The objectives of the present study are to: 1) use field and micromorphological descriptions of paleosols and paleoenvironmental proxies or pedotransfer functions derived from their bulk geochemical composition to reconstruct a series of paleocatenas at Kisaaka; 2) provide context for faunal and archeological records at Kisaaka; and 3) integrate paleoprecipitation estimates into the regional paleoclimate and paleoenvironment of the late Pleistocene in equatorial East Africa to quantify some of the factors that may have contributed to human evolution and dispersal in the late Pleistocene.

Background

Lake Victoria basin

Lake Victoria is the largest freshwater lake in the tropics by surface area (~66,400 km^2), spanning the equator in a depression between the eastern and western branch of the East African Rift System (EARS). The lake is very shallow with a maximum depth of ~68 m (Stager and Johnson, 2008) in comparison to the other African Great Lakes, lakes

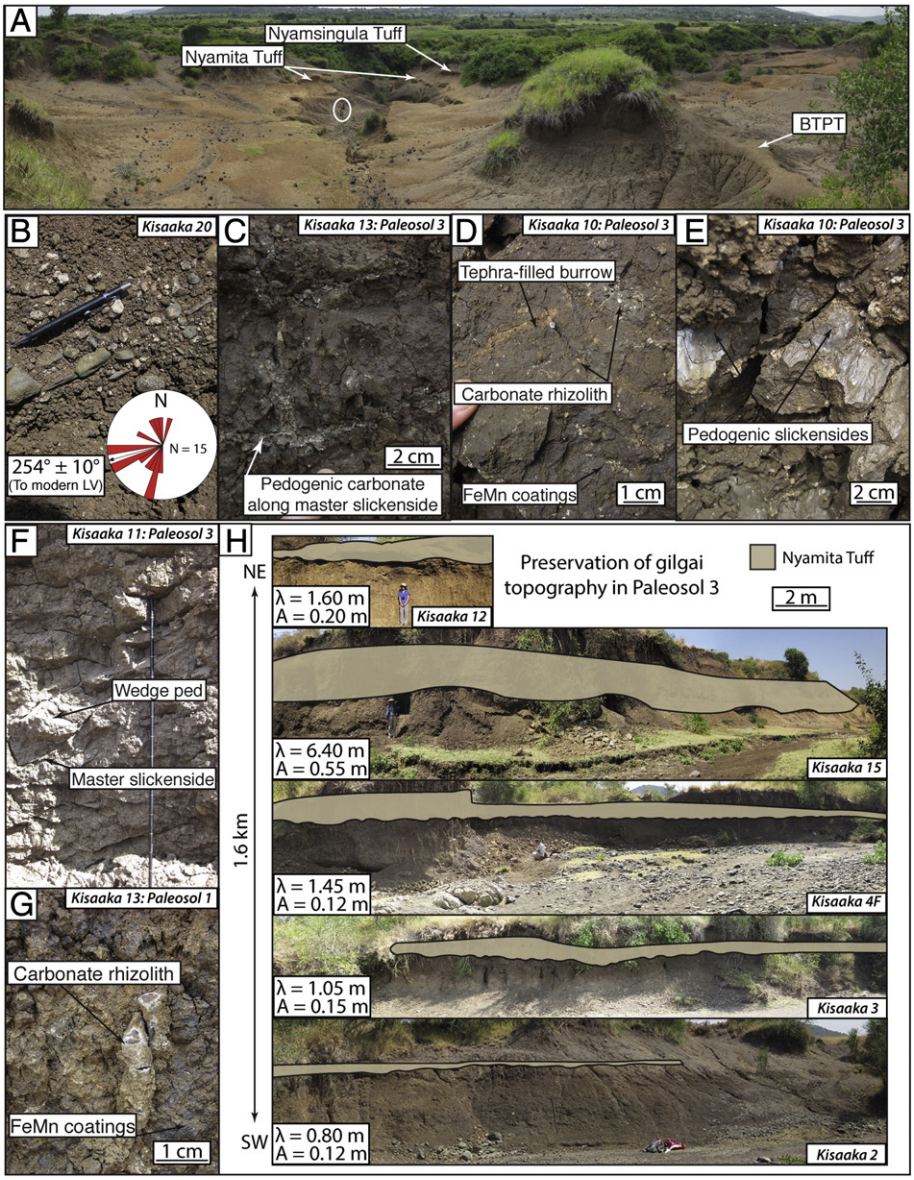

Figure 3. Field photos of key features described in Fig. 2. See Fig. 1 for location. A) Panoramic view of Kisaaka 13 with correlative tuffs identified and person circled for scale. B) Imbricated cobbles used to determine a mean paleocurrent direction of 254°N flowing towards modern Lake Victoria. C) Paleosol 3: Pedogenic carbonate precipitating along a master slickenside. D) Top view Paleosol 3: Tephra filled burrows, carbonate rhizoliths, and FeMn coatings visible. E) Paleosol 3: Well-developed pedogenic slickensides. F) Paleosol 3: Extremely well-developed vertic features with wedge peds and master slickenside. G) Paleosol 1: Carbonate rhizoliths and FeMn coatings are visible with subangular blocky peds. Representative of both Paleosols 1 and 2. H) Preservation of gilgai topography due to deposition of Nyamita Tuff. λ = wavelength of gilgai. A = amplitude of gilgai.

https://doi.org/10.1016/j.yqres.2015.08.002 Published online by Cambridge University Press

Malawi and Tanganyika, which are 700 and 1470 m deep, respectively (Bootsma and Hecky, 2003). Lake Victoria likely began to form between ~1.6 and ~>0.4 Ma when uplift associated with the western arm of the EARS began to dam westward-flowing rivers, causing ponding between the western and eastern arms of the EARS (Kent, 1944; Doornkamp and Temple, 1966; Bishop and Trendall, 1967; Ebinger, 1989; Johnson et al., 1996; Talbot and Williams, 2009).

The Intertropical Convergence Zone (ITCZ) is the primary control on precipitation in the Lake Victoria region, which today crosses the region twice a year bringing long rains in March and shorter rains in October (Song et al., 2004). Mean annual precipitation (MAP) at Mbita, Kenya, which is proximal to the study area (Fig. 1B), is ~1400 mm yr^{-1} (Crul, 1995; Fillinger et al., 2004). Up to 80% of the water input is from direct precipitation on the lake surface, and most of the water loss (up to 90%) is from evaporation (Crul, 1995). Thus, small changes in precipitation likely have a significant influence on water input and lake volume (Broecker et al., 1998; Milly, 1999).

Geological evidence suggests that Lake Victoria increased in size compared to present surface area and desiccated multiple times, with the most recent desiccation occurring at 15 ka (Heinrich Event 1) (Johnson et al., 1996; Talbot and Laerdal, 2000; Stager et al., 2002, 2011). The desiccation at 16 ka led to the formation of a paleo-Vertisol across much of the basin that has been identified in multiple cores across Lake Victoria, but none of the cores penetrated more than a few cm beneath the paleo-Vertisol (Johnson et al., 1996; Stager et al., 2002, 2011). This 15 ka paleo-Vertisol surface can be identified in seismic profiles across the entire lake basin, and similar underlying surfaces identified in the seismic data suggest that the lake desiccated multiple times prior to Heinrich Event 1 (Johnson et al., 1996; Stager et al., 2002, 2011).

Karungu

Karungu (0.84°S, 34.15°E) is located on the Kenyan margin of Lake Victoria (Fig. 1), ~40 km south of Pleistocene localities on Rusinga and Mfangano Islands that have been the focus of research by our team since 2009 (Tryon et al., 2010; Faith et al., 2011; Van Plantinga, 2011; Faith et al., 2012; Tryon et al., 2012; Faith et al., 2014; Tryon et al., 2014; Beverly et al., 2015; Garrett et al., 2015). The Pleistocene deposits at Karungu are exposed at seven sites around the town of Sori. They were originally noted by Owen (1937) and mapped by Pickford (1984). The best-exposed sites (Kisaaka, Aringo, Onge, Obware, and Aoch Nyasaya) were further investigated and mapped in greater detail by Beverly et al. (2015), Faith et al. (2015), and Blegen et al. (2015). The Kisaaka locality has the most laterally extensive (~2 km) and thickest (2.5 to 11 m) outcrops at Karungu, and the paleosols identified in these deposits are the focus here (Fig. 3A). The stratigraphy varies across Kisaaka, but generally, freshwater tufa that precipitated on Miocene bedrock composed of conglomerates and breccias forms the base of the sequence and is overlain by conglomerates, paleosols, and tuffaceous sediments (Beverly et al., 2015; Blegen et al., 2015; Faith et al., 2015).

There are five compositionally distinct tuffs exposed at Kisaaka. As a result of a comprehensive program of geochemical characterization involving electron microprobe analyses of 50 samples, the tuffs at Karungu can be correlated with those to the north at Rusinga and Mfangano Islands where they have been dated by multiple radiometric methods (Tryon et al., 2010; Van Plantinga, 2011; Beverly et al., 2015; Blegen et al., 2015; Faith et al., 2015; Garrett et al., 2015). As summarized in Figure 2, the lowermost tephra, the Wakondo Tuff and an unnamed rhyolitic tuff were deposited between ~94 and 49 ka based on U-series dating of the underlying tufa (Beverly et al., 2015) and OSL ages on overlying sands (Blegen et al., 2015; Faith et al., 2015). The Nyamita Tuff was deposited at ~49 ka based on OSL ages on sand deposits bracketing the tephra (Blegen et al., 2015; Faith et al., 2015). The Nyamsingula Tuff is overlain by the Bimodal Trachyphonolitic Tuff (BTPT), and both were dated between >49 and 33 ka based on their stratigraphic relationship with the underlying Nyamita Tuff and AMS radiocarbon ages on gastropod shells that post-depositionally burrowed into the sediment (Tryon et al., 2010; Blegen et al., 2015). These gastropods (*Limicolaria* cf. *martensiana*) are only found in the upper sediments in life position and therefore provide a minimum age for these deposits.

At Kisaaka, three paleosols are identified (Fig. 2), separated by tuffs that allow their correlation over a ~2 km transect and preserve the topography of the paleocatenas. The Nyamita Tuff, the Nyamsingula Tuff, and the BTPT Tuff can be laterally traced between numerous outcrops across Kisaaka, with additional correlations among discontinuous exposures confirmed on the basis of geochemical composition (Blegen et al., 2015; Faith et al., 2015). Two outcrops preserve the entire stratigraphic sequence (Kisaaka 10 and 13; Fig. 1C). Kisaaka 13 is the representative section for the stratigraphic sequence at Kisaaka (Figs. 2 and 3A). From bottom to top, Kisaaka 13 has a 2 m-thick paleosol (Paleosol 3) that is overlain by 1 m of the Nyamita Tuff. Above the Nyamita Tuff is a thin (0.8 m) paleosol unit capped by the Nyamsingula Tuff, which is designated Paleosol 2. The youngest paleosol, designated Paleosol 1, is 2.2 m thick and is overlain by the BTPT Tuff.

Methods

In order to use the Kisaaka paleosols to infer past environmental conditions, all outcrop locations were recorded and mapped using hand-held GPS (Supplementary Table 1), the exposures were trenched to expose bedding unaffected by modern processes, and the stratigraphic sequence measured and described at the cm scale. All lithologic and pedogenic features were recorded and photographed. Wavelength and amplitude of gilgai topography, typical of soils affected by shrinking and swelling of clays, were measured in the field and averaged by location for comparison across the landscape. Paleocurrent measurements on imbricated cobbles were collected from seven locations. Samples were collected for bulk geochemistry and clay mineralogy at 10 cm vertical intervals through the paleosols, and where applicable, samples were collected from gilgai topography micro-lows where erosion is less likely and pedogenic processes are greatest (Driese et al., 2000, 2003). Oriented samples for micromorphological analysis were collected from each identified soil horizon.

Samples were pulverized for mineralogical and geochemical analysis. Paleosol mineralogical analysis was conducted at Baylor University on a Siemens D-5000 θ–2θ X-ray diffractometer (XRD) using Cu Kα radiation at 40 Kv and 30 mA. Samples were scanned from 2 to 60° 2θ, at a 0.05° step per 1.5 s for bulk powder and <2 μm fraction of four oriented aggregate treatments (MgCl, MgCl plus glycerol, KCl at 25°C, KCl heated to 550°C for 24 h) using the Millipore system described in Moore and Reynolds (1997).

Bulk geochemical samples were sent for commercial analysis to ALS Geochemistry (Reno, NV) for major, rare, and trace element analyses using a combination of inductively coupled plasma atomic emission spectroscopy (ICP-AES) and inductively coupled plasma mass spectrometry (ICP-MS). The complete geochemical analyses of all samples are available in Supplementary Table 2. All bulk geochemical data were normalized to molecular weight for application to molecular weathering ratios and pedotransfer functions developed to reconstruct soil properties of paleo-Vertisols after Retallack (2001) and Nordt and Driese (2010a), respectively. Molecular weathering ratios were considered to examine relative changes in weathering such as hydrolysis or salinization down profile (Retallack, 2001). Pedotransfer functions were developed to relate the bulk geochemistry of paleosols to physical and chemical properties determined by the USDA-NRCS using regression based transfer functions (Nordt and Driese, 2010a).

Bulk geochemical data were also used to calculate paleoprecipitation using the chemical index of alteration minus potassium (CIA-K) for all soil types (Sheldon et al., 2002), and the CALMAG proxy, specific to paleo-Vertisols (Nordt and Driese, 2010b). CIA-K is defined as Al_2O_3/

https://doi.org/10.1016/j.yqres.2015.08.002 Published online by Cambridge University Press

$(Al_2O_3 + CaO + Na_2O) \times 100$ and is a weathering index that measures clay formation and base loss associated with feldspar weathering and was designed to be universal for all paleosol types in which there has been sufficient time of soil formation to equilibrate with climate conditions (Sheldon et al., 2002). The application of the CIA-K proxy to Vertisols can be problematic because CIA-K measures the hydrolysis of weatherable minerals, and hydrolysis in Vertisols is very limited due to the stability of the smectite and illite clay minerals. The smectitic clay is often pre-weathered in Vertisols due to inheritance of clays from the parent material. Therefore, the CALMAG weathering index was developed specifically for paleo-Vertisols, which is defined as $Al_2O_3/(Al_2O_3 + CaO + MgO) \times 100$ where all oxides are normalized to their molar ratios. CaO and MgO accounts for 90% of the variation with climate in Vertisols and therefore MgO is substituted for Na_2O. This substitution also reduces the influence of primary sodium-bearing minerals. The CIA-K and CALMAG weathering indices in modern soils have a strong correlation to MAP and these indices can be used to estimate paleo-rainfall using stepwise linear regression.

Nineteen thin-sections were prepared commercially by Spectrum Petrographics, Inc. Oriented samples were stabilized in the field and lab with epoxy and then vacuum-impregnated with epoxy prior to thin section preparation. Micromorphological study of paleosols was conducted at Baylor University using techniques established by Fitzpatrick (1993) and Stoops (2003) on an Olympus BX-51 polarized-light microscope equipped with a 6.5 MPx Leica digital camera and an ultraviolet fluorescence (UVf) attachment. Changes in organic matter content were visually estimated by subjecting the thin section to UVf causing the organic matter to autofluoresce. Photomicrographs of unique and representative features were taken using three different UVf wavelength filters, NU, NB, and TXRED, in addition to those taken with cross-polarized light (XPL) and plane-polarized light (PPL).

Results

Field and micromorphological descriptions

Of the sequence of three paleosols at Kisaaka, Paleosol 3 is the easiest to identify and correlate because the Nyamita Tuff forms a thick, locally distinctive marker bed that caps it throughout the Kisaaka locality (Figs. 2 and 3H). Paleosol 3 varies in thickness from 1.5 to 3.5 m, and where the base of the stratigraphy is exposed, it overlies a tufa-cemented conglomerate, the rhyolitic tuff, or the Wakondo Tuff. This conglomerate is part of a fining upward sequence and is often imbricated allowing for paleocurrent measurements (Fig. 3B). The measurements indicate that the paleoflow direction was generally to the west (N 254° ± 10°) in the direction of modern Lake Victoria, paralleling modern drainage patterns. Paleosol 3 is identified as a paleo-Vertisol in outcrop by the medium to coarse wedge peds, pedogenic slickensides with angles up to 45°, master slickensides, and gilgai topography (Fig. 3C–F, H). The wavelength (λ) and amplitude (A) of these gilgai varies significantly across the landscape (Fig. 3H). At the northeast (Kisaaka 12) and southwest (Kisaaka 2, 3, and 4 F), the average λ ranges from 0.8 to 1.6 m and the average A ranges from 0.12 to 0.20 m. At the Kisaaka 15 site, the average λ is 6.4 m and the average A is 0.55 m.

Vertic features are also present in thin section. The oriented birefringent clay (b-fabric) is identified as pedogenic slickensides in the micromorphology (Fig. 4B) by the lack of laminations and identical grain size between oriented clay and the matrix (Stoops et al., 2010). This is best illustrated by contrasting the oriented clay in XPL and PPL (Fig. 4B). Parallel striated and granostriated b-fabrics are also common in the Bkss horizons and with some areas of more developed cross-striated b-fabric (Table 1).

The type section for Paleosol 3 is divided into five soil horizons: ABkb3, Bkb3, Bkss1b3, Bkss2b3, and Bkss3b3 that are described in detail in Table 1. At some sites, the A horizon, characterized by granular peds, has been eroded (Kisaaka 4F). In other areas the paleo-Vertisol is significantly thicker (Kisaaka 14A) or thinner (Kisaaka 4F or 12), but the paleosol has remarkably similar features across the landscape (Fig. 2). The paleo-Vertisol contains both carbonate nodules and rhizoliths throughout the profile (Figs. 2, 3D, and 4A). The carbonate rhizoliths are commonly poorly developed and powdery, but the nodules are dense micrite with septarian and circumgranular cracks (Fig. 4A). Carbonate was also identified along ped boundaries especially master slickenside surfaces (Fig. 3C). Rhizocretions are also identified in the lower horizons (Fig. 2). Throughout the paleo-Vertisol are tephra-filled burrows often associated with fecal pellets that are likely attributed to earthworms due to their size (200–500 μm) (Figs. 2, 3D, and 4C; Stoops et al., 2010). Burrows with meniscate backfill were also identified in thin section and can also be attributed to earthworms (Fig. 4C; Stoops et al., 2010).

Paleosol 2 overlies the Nyamita Tuff and has 4 soil horizons: Bk1b2, Btk1b2, Btk2b2, and Bk2b2. This is a paleo-Inceptisol with Alfisol-like soil characteristics, but the lack of E horizon prevents classification as an Alfisol (Soil Survey Staff, 1999). In outcrop, this paleosol is thin (40–80 cm) and poorly developed with only granular to subangular blocky peds, FeMn coatings on peds, tephra-filled burrows, and weakly developed pedogenic carbonate nodules and rhizoliths (Fig. 3G). In thin section, the carbonate often has diffuse boundaries filling in pore spaces and engulfing paleosol matrix. The micromorphology also reveals a much more complex pedogenesis with abundant illuviated clay coatings of up to 3% in the Btk1b2 and Btk2b2 horizons (Fig. 4H). These coatings were not visible in outcrop because the majority of the coatings are covered with a second layer of FeMn that prevented field identification (Figs. 3G, 4G, and J).

MSA artifacts have been collected from the surface at Kisaaka, but systematic excavations have yet to be conducted and few artifacts have been found in situ at this site (Faith et al., 2015). Paleosol 2 has evidence for microdebitage from on-site tool production where several large, angular grains of chert have been identified (Fig. 4K). Artifacts made from this material were collected at Kisaaka (Faith et al., 2015). These grains are much larger than the dominantly silt- to fine sand-sized coarse fraction and contain percussion fractures typical of microdebitage (Angelucci, 2010).

Paleosol 1 is a paleo-Inceptisol with Alfisol-like soil characteristics, like Paleosol 2. Paleosol 1 is thicker (2.2 m) and better developed and has 4 horizons: ABkb1, Btkb1, Btk2b1, and BC1b1 (Table 1). The ABkb1 horizon contains granular peds and all other horizons are dominated by subangular blocky peds (Fig. 4G). FeMn coatings, tephra-filled burrows (Fig. 4D), carbonate rhizoliths are abundant throughout the profile (Figs. 3G, 4D, and H). Similar to Paleosol 2, the micromorphology reveals an abundance of features not visible in outcrop due to the abundance of FeMn coatings. Earthworm fecal pellets (~500 μm) are present throughout the matrix and commonly fill burrows (Fig. 4E). These burrows generally allowed for preferential flow and greater accumulations of illuviated clay (Fig. 4D, E, and F). Much smaller fecal pellets (50–100 μm) are also preserved in carbonate rhizoliths (Fig. 4H and I) and were likely made by termites, which produce fecal pellets ~100 μm in diameter (Jungerius et al., 1999; Stoops et al., 2010). The carbonate rhizoliths and nodules are poorly developed in comparison to Paleosol 3 and often have diffuse boundaries (i.e. Fig. 4A vs. D and H). In addition, coatings on pores crosscutting relationships record the time of features: 1) illuviated clay; 2) FeMn coatings; and 3) carbonate (Fig. 4G and J). The illuviated clay coatings are well developed and comprise up to 5% of the paleosol in the Btk2b1 horizon (Fig. 4G). In some areas, pores have multiple generations of illuviation and >10 bands of illuviated clay, which range from 5 to 10 μm in width (Fig. 4F and L).

Mineralogy

Mineralogy of paleosols was analyzed by horizon but showed little variability, and therefore only examples from Paleosols 1 and 3 are

https://doi.org/10.1016/j.yqres.2015.08.002 Published online by Cambridge University Press

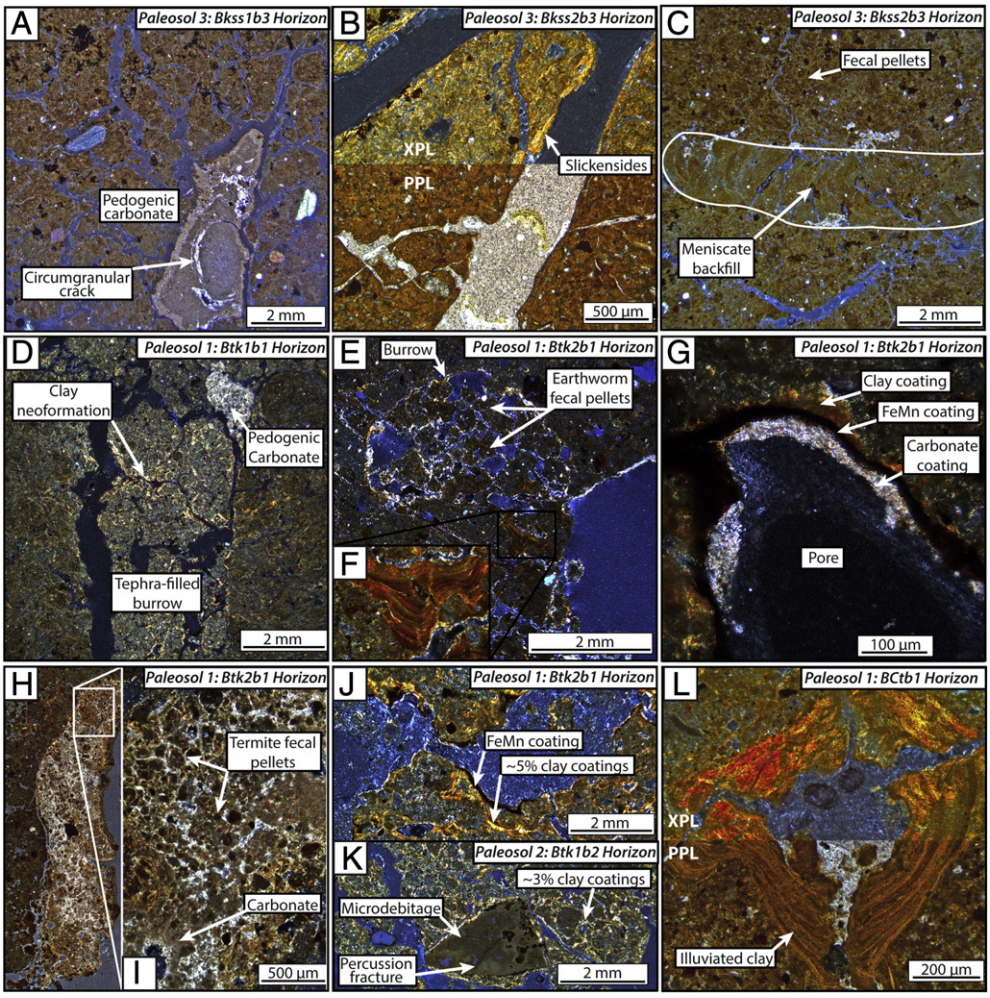

Figure 4. Photomicrographs of representative microstructures and biologic features. All photomicrographs are oriented vertically. A) Paleosol 3: Very different soil matrix with little tephra, but very well developed pedogenic carbonates with circumgranular cracking, 1.25× XPL. B) Paleosol 3: Pedogenic slickensides, 4×, upper XPL, lower PPL. C) Paleosol 3: Fecal pellets in the matrix and a burrow with meniscate backfill, 1.25× XPL. D) Paleosol 1: Burrow filled with tephra undergoing neoformation to clay and pedogenic carbonate, 1.25× XPL. E) Paleosol 1: Burrow filled with fecal pellets, likely by earthworms, and illuviated clay, 1.25× XPL. F) Paleosol 1: Close up of illuviated clay, 10× XPL. G) Paleosol 1: Cross-cutting relationships of pedogenic features: 1) illuviated clay; 2) FeMn; and 3) carbonate, 20× XPL. H) Paleosol 1: Carbonate rhizolith, 1.25× XPL. I) Paleosol 1: Close-up of fecal pellets, likely from termites, cemented by calcite in rhizolith, 4× XPL. J) Paleosol 1: Illuviated clay (~5%) and FeMn coatings filling pore spaces and coating ped surfaces, 1.25× XPL. K) Paleosol 2: ~3% Illuviated clay coating ped surfaces and microdebitage, 1.25× XPL. L) Paleosol 1: Very well-developed illuviated clay with at least ten generations of illuviation, 10×, upper XPL, lower PPL.

included here. Sample locations are shown on Figure 2. Figure 5A is representative of Paleosols 1 and 2 (Inceptisols) and Fig. 5B is representative of Paleosol 3 (Vertisols). All paleosols contain abundant smectite with variable contributions of palygorskite, quartz, feldspar, and augite. The broad 16.6 Å peaks are indicative of poorly crystalline smectite (Fig. 5B), and the weak intensities in the upper paleosols are attributed to the abundance of amorphous tephra (Fig. 5A).

Bulk geochemistry

Bulk geochemistry is commonly used to determine paleosol weathering trends with depth using molecular weathering ratios, and constitutive mass balance models have been used in the past to quantify these changes (Brimhall and Dietrich, 1987; Chadwick et al., 1990; Sheldon and Tabor, 2009). Mass balance is a powerful tool because it compares the ratio of the weathered material to the parent material and takes into account changes in bulk density (Brimhall and Dietrich, 1987; Chadwick et al., 1990). When bulk density is not accounted for, increasing porosity can have the effect of making it appear that the ratio of weathered material to the parent material is constant (Brimhall and Dietrich, 1987; Chadwick et al., 1990). However, all Kisaaka paleosols were weathered throughout the profile leaving no unweathered parent material to calculate mass balance. Molecular weathering ratios can only be used to examine relative changes down profile for an individual paleosol because the molecular weathering ratios do not account for parent material and density changes (Retallack, 2001). For this reason, it is difficult to compare between paleosols and across the landscape and through time using molecular weathering ratios. There is little change in parent material across the landscape, but density can fluctuate significantly due to varying contributions of tephra. The geochemistry of the Kisaaka paleosols show little consistent variability with depth likely due to the limitations of molecular weathering ratios rather than a lack of weathering due to insufficient pedogenesis. Therefore, the bulk geochemistry has been averaged by paleosol, in addition to the molecular weathering ratios and paleoprecipitation proxies calculated from the bulk geochemistry, to show general trends between paleosols and across the landscape (Table 2). All paleosols show evidence of pedogenesis, seen by comparing the additions of CaO, MgO, and Fe_2O_3 and losses of Na_2O in the paleosols to the bulk geochemistry of Nyamsingula and Nyamita tuffs, which are possible parent materials (Table 2). Paleosols 1 and 2 show no variability across the landscape, but Paleosol 3 indicates some variability, such that paleosols at Kisaaka 10 and Kisaaka 13 have higher CaO and lower Fe_2O_3 and Al_2O_3 in comparison to the paleosols at the

https://doi.org/10.1016/j.yqres.2015.08.002 Published online by Cambridge University Press

Table 1
Summary of field and micromorphological descriptions of type section paleosols at Kisaaka 13.

Horizon	Munsell color	Pedogenic features	Illuviated clay (%)	B-fabric	Biologic indicators
Paleosol 1: Inceptisol (49 to >33)					
ABkb1	10YR 5/4	• Granular and subangular blocky peds • FeMn redoximorphic redistribution in matrix • Poorly developed carbonate nodules often with diffuse boundaries	<1	None	• Earthworm fecal pellets • Tephra filled burrows • Carbonate rhizoliths
Btk1b1	10YR 5/3	• Subangular blocky peds • FeMn coatings on peds and redoximorphic redistribution in matrix • Poorly developed carbonate nodules often with diffuse boundaries	3	None	• Earthworm fecal pellets • Tephra filled burrows • Carbonate rhizoliths
Btk2b1	10YR 4/2.5	• Subangular blocky peds • FeMn coating on peds and minor redoximorphic redistribution in matrix • Poorly developed carbonate nodules often with diffuse boundaries • Complex history of FeMn, illuviated clay, and carbonate coatings in pores • Pedorelicts	5	None	• Abundant earthworm fecal pellets • Tephra filled burrows, often preferential flowpath for illuviated clay • Carbonate rhizoliths • OM complexed with illuviated clay and disseminated in matrix
BCtb1	10YR 5/4	• Angular blocky peds • Complex history of FeMn, illuviated clay, and carbonate coatings in pores • Tephra increases with depth throughout profile and gradual boundary with Nyamsingula Tuff	3	None	• Abundant earthworm fecal pellets but forming dense microaggregates • Tephra filled burrows • Carbonate rhizoliths
Paleosol 2: Inceptisol (49 to >33)					
Bk1b2	10YR 5/4	• Granular to subangular blocky peds • FeMn coating on peds	<1	None	• Earthworm fecal pellets • Tephra filled burrows • Weakly developed carbonate rhizoliths
Btk1b2	10YR 4/3	• Subangular blocky peds • FeMn coating on peds • Complex history of FeMn, illuviated clay, and carbonate coatings in pores • Pedorelicts • Weakly developed pedogenic slickensides	3	None	• Earthworm fecal pellets • Tephra filled burrows • Weakly developed carbonate rhizoliths • Microdebitage
Btk2b2	10YR 5/4	• Subangular blocky peds • FeMn coatings on peds • Poorly developed carbonate nodules often with diffuse boundaries • Complex history of FeMn, illuviated clay, and carbonate coatings in pores • Pedorelicts	3	None	• Earthworm fecal pellets • Tephra filled burrows • Weakly developed carbonate rhizoliths
Bk2b2	10YR 4/3	• Subangular blocky peds • FeMn coatings on peds • Gradual boundary with Nyamita Tuff • Stone line	<1	None	• Bone fragment • Weakly developed carbonate rhizoliths
Paleosol 3: Vertisol (94 to 49 ka)					
ABkb3	10YR 4/3	• Granular to subangular blocky peds • FeMn coatings on peds	0	None	• Tephra filled burrows • Weak to well developed carbonate rhizoliths
Bkb3	10YR 4/2	• Angular blocky peds • FeMn coatings on peds • FeMn glaebules • Tephra weathering to clay but no indication of illuviation	0	Parallel to weakly cross-striated, granostriated	• Earthworm fecal pellets • Tephra filled burrows • Weak to well developed carbonate rhizoliths
Bkss1b3	10YR 3/2	• Subangular blocky and wedge peds • Pedogenic slickensides • FeMn coatings on peds and redoximorphic redistribution in matrix • Well-developed carbonate nodules with septarian and circumgranular cracks • Tephra weathering to clay but no indication of illuviation	0	Parallel to granostriated	• Earthworm fecal pellets • Tephra filled burrows • Weak to well developed carbonate rhizoliths
Bkss2b3	10YR 3/2	• Subangular blocky and wedge peds • Pedogenic slickensides • Carbonate along master slickensides • FeMn coatings on peds and redoximorphic redistribution in matrix • Carbonate nodules	0	Parallel striated	• Tephra filled burrows • Carbonate rhizoliths and rhizocretions • Burrows with meniscate backfill
Bkss3b3	10YR 4/2	• Subangular blocky and wedge peds • Pedogenic slickensides • Carbonate nodules	0	Granostriated	• Tephra filled burrows • Carbonate rhizoliths and rhizocretions • Burrows with meniscate backfill

Kisaaka 4F and 12 localities (Table 2). There is also very little variability through time between Paleosols 1, 2, and 3 with the exception of CaO and leaching, which is calculated using CaO content in the paleosols.

Pedotransfer functions were applied to the paleosols with vertic features (Paleosol 3 only) to reconstruct colloidally based physical and chemical properties used in modern soil characterization (Nordt and

https://doi.org/10.1016/j.yqres.2015.08.002 Published online by Cambridge University Press

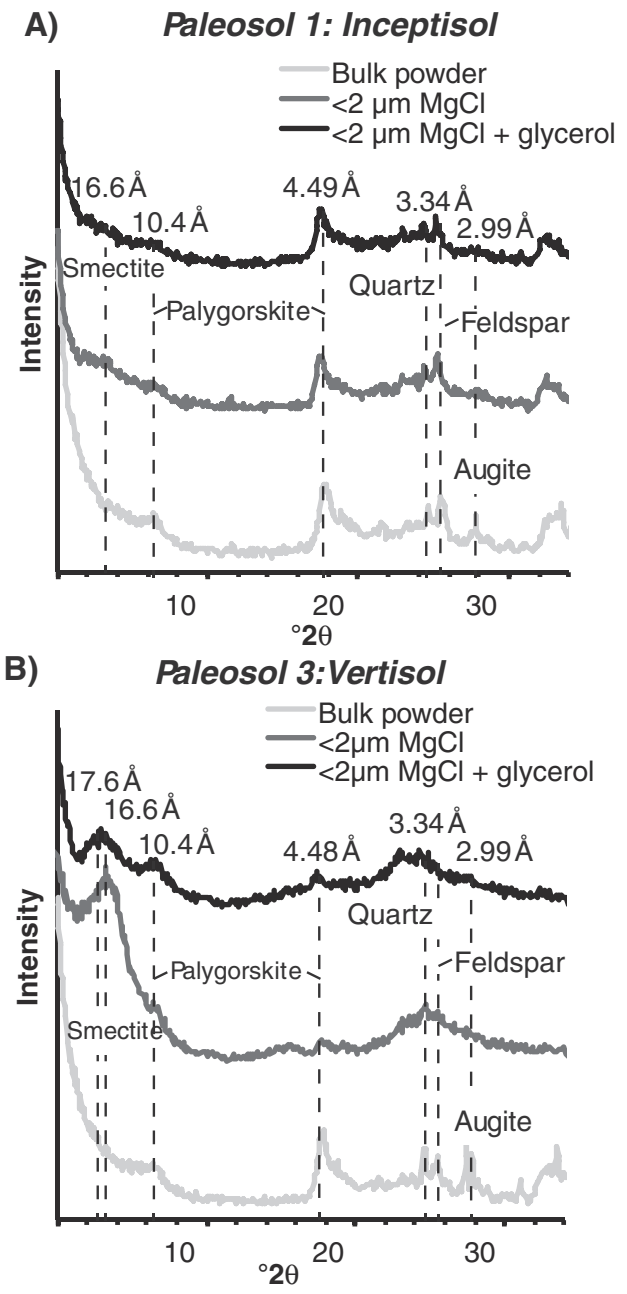

Figure 5. Clay mineralogy of paleosols. The abundance of poorly crystalline tephra within this paleosol created poorly defined peaks and made identification difficult. A) Clay mineralogy of Paleosol 1 that is representative of both Inceptisols 1 and 2. Dominated by poorly crystalline smectite and palygorskite with minor amounts of quartz and augite. B) Paleosol 3 dominated by smectite with minor amounts of palygorskite, quartz, and augite.

Driese, 2010a). Some pedotransfer functions developed by Nordt and Driese (2010a) were not applicable due to the presence of carbonate and only those applicable are presented here: total clay, fine clay, the ratio of fine clay to total clay (FC/TC), coefficient of linear extensibility (COLE), cation exchange capacity (CEC), the ratio of CEC to clay (CEC/clay), pH, base saturation (BS), exchangeable sodium percentage (ESP), electrical conductivity (EC), crystalline Fe oxide (Fe_d), and percent $CaCO_3$. These properties all yield further information on soil fertility and are summarized in Table 3. Detailed explanation of these modern soil properties can be found in Burt (2011).

The ratio of FC/TC indicates no translocation with depth, paralleling observations in the field and in thin section (Tables 1 and 2). The high proportion of clay and specifically smectitic clay (Fig. 5B) gives the paleosols a high shrink-swell potential, high COLE of 0.07 to 0.09 cm cm^{-1} (high is defined as 0.06 to 0.09 cm cm^{-1} by the NRCS (Burt, 2011), and high CEC between 30.7 and 44.2 cmolc kg^{-1} (Table 3). The CEC is the total number of exchangeable cations that a soil can absorb and depends on the types of clays and amount of organic matter present in the soil that hold these exchangeable cations (Brady and Weil, 2008). Smectite has a high CEC (~80 to 130 cmolc kg^{-1}) and for this reason modern Vertisols often have a high CEC of ~-35.6 cmolc kg^{-1} (Brady and Weil, 2008). Base saturation (BS) is a measure of how many base cations the soil potentially holds (Brady and Weil, 2008), and the Kisaaka paleosols are all base saturated at 99 to 100%. A higher pH also increases the effective CEC and the Kisaaka paleosols have alkaline pH of between 7.4 and 8.2. The CEC, BS and pH are all buffered by the presence of carbonate, which ranges from 3 to 11%, with the highest carbonate at Kisaaka 13 and the lowest at Kisaaka 4F and 12 (Table 3). ESP is a measure of the sodicity of the soil, which affects both physical and chemical soil properties that are detrimental to plant growth. A soil classified as normal has an ESP of <15% and indicates that plants with a typical tolerance will be unaffected by sodicity. All but the upper horizons in Kisaaka 12 have an ESP > 10%, and most horizons are >15%. The Fe_d is often used as a measure of total pedogenic Fe from minerals such as goethite, hematite, lepidocrocite, and ferrihydrite and with >1% indicative of oxidizing soil conditions (Nordt and Driese, 2009, 2010a). The Fe_d ranges from 8 to 14% in Paleosol 3 (Table 3).

Paleoprecipitation was also calculated using CALMAG for those paleosols identified as Vertisols (Paleosol 3) and CIA-K for all paleosols. The paleoprecipitation estimates for Paleosol 3 averages 764 ± 108 and 823 ± 182 mm yr^{-1} for CALMAG and CIA-K, respectively. Paleosol 2 is higher with an average of 963 ± 182 mm yr^{-1} and Paleosol 1 has an average of 813 ± 182 mm yr^{-1} (Table 2).

Discussion

Depositional environment

The three laterally continuous tuffs deposited at Kisaaka (the Nyamita Tuff, the Nyamsingula Tuff, and the BTPT) preserve a succession of buried landscapes and allow for the reconstruction three separate paleocatenas. The Kisaaka paleosols often have a similar grain size (clay-sized) throughout the profile, few erosive scour surfaces, and well-developed pedogenic features. Paleosols with these features often form in a fluvial system, distal to the active fluvial channel, with steady depositional conditions where pedogenesis is able to keep up with constant additions and forming well-developed, but cumulative soils (Kraus, 1999).

Gilgai topography

The oldest and best preserved paleocatena (Paleosol 3), formed between 94 and ~49 ka, is a paleo-Vertisol with pedogenic slickensides (Fig. 5E) that are indicative of intensive shrink-swell processes due to wetting and drying of smectite (Fig. 5B). The shrinking and swelling of the clay during wet and dry seasons formed gilgai topography that is preserved by the rapid deposition of the Nyamita Tuff at ~49 ka. Gilgai topography is rarely preserved in the rock record as the granular peds of the A horizon are easily eroded prior to the next depositional event and eroding the gilgai topography in the process (Caudill et al., 1996; Mora and Driese, 1999; Driese et al., 2000, 2003). The wavelengths and amplitudes of these well-preserved gilgai vary across the landscape and may reflect changes in gilgai type. The wavelengths and amplitudes of gilgai identified at the Kisaaka 12, 4F, 3, and 2 localities (Fig. 3H) ranges from 0.8 to 1.6 m. In comparison, the average wavelength from Kisaaka 15 is much larger at 6.4 m with amplitudes of 0.55 m on average. These large wavelengths and amplitudes can form in linear gilgai that form on sloping landscapes, commonly, 1° to 3° (Hallsworth

https://doi.org/10.1016/j.yqres.2015.08.002 Published online by Cambridge University Press

Table 2
Average bulk geochemistries of paleosols and tephra in wt%, average of molecular weathering ratios normalized to molecular weight, and averaged by paleosol.

Locality	Unit	Al_2O_3	CaO	MgO	Na_2O	K_2O	SiO_2	BaO	SrO	Fe_2O_3	Leaching	Salinization	Hydrolysis	Hydration	CALMAG (mm/yr) SE ± 108	CIA-K (mm/yr) SE ± 182
10	Paleosol 1	13.16	2.51	2.35	1.38	2.12	45.68	0.06	0.04	13.27	1.06	0.17	0.17	3.59	–	725
13	Paleosol 1	13.36	3.04	2.24	2.12	2.51	49.75	0.07	0.05	11.09	0.98	0.26	0.16	4.13	–	901
	Average	**13.26**	**2.78**	**2.29**	**1.75**	**2.31**	**47.72**	**0.07**	**0.05**	**12.18**	**1.02**	**0.22**	**0.16**	**3.86**	–	**813**
10	Paleosol 2	14.44	1.37	1.89	1.81	2.46	50.28	0.05	0.03	11.19	1.14	0.21	0.17	3.96	–	987
13	Paleosol 2	14.06	1.56	2.08	2.18	2.46	51.94	0.05	0.04	10.83	0.94	0.26	0.16	4.21	–	939
	Average	**14.25**	**1.47**	**1.98**	**1.99**	**2.46**	**51.11**	**0.05**	**0.03**	**11.01**	**1.04**	**0.23**	**0.16**	**4.08**	–	**963**
4F	Paleosol 3	13.44	3.67	2.39	1.60	2.22	45.95	0.16	0.05	14.41	1.88	0.20	0.17	3.44	812	726
10	Paleosol 3	12.21	5.00	2.16	1.18	2.13	46.16	0.11	0.05	11.54	1.55	0.16	0.16	4.01	840	915
13	Paleosol 3	12.82	5.09	2.46	1.88	2.21	44.80	0.11	0.05	13.02	1.33	0.24	0.17	3.59	579	685
12	Paleosol 3	13.53	2.38	2.80	1.22	2.20	47.42	0.07	0.05	14.62	1.06	0.15	0.17	3.52	826	967
	Average	**13.00**	**4.03**	**2.45**	**1.47**	**2.19**	**46.08**	**0.11**	**0.05**	**13.40**	**1.46**	**0.19**	**0.17**	**3.64**	**764**	**823**
10	Nyamsingula Tuff	13.3	1.47	1.66	2.26	2.54	52.7	0.07	0.04	10.65	–	–	–	–	–	–
10	Nyamita Tuff	14.95	1.15	1.79	2.36	2.59	49.2	0.05	0.03	10.95	–	–	–	–	–	–

– not applicable.

et al., 1955; Hallsworth and Beckman, 1969; Beckmann et al., 1970, 1973).

Linear gilgai are commonly identified in Australia (Hallsworth and Beckman, 1969; Beckmann et al., 1973), but are rare in Africa or not reported in the literature. Examples of both normal and linear gilgai have been identified at Rustenburg, South Africa, and the normal gilgai have shorter wavelengths of ≤5 m, but the linear gilgai have wavelengths of ≥8 m (Verster et al., 1973; Fey et al., 2010). This suggests that specific conditions may be needed to form these features. The physical and colloidal soil properties of the modern Rustenburg Vertisols with 62% to 69% clay, a CEC of 34 to 58, pH of 7.7 to 8.6, and a range of carbonate from 0 to 15.5% are remarkably similar to those reconstructed using pedotransfer functions for the Kisaaka paleo-Vertisols (Table 2; Verster et al., 1973). This suggests that the Kisaaka paleotopography may have been similar to Rustenburg where specific conditions allow for gilgai formation. Seasonal rainfall ranging from 600 to 700 mm yr^{-1}, and the smectitic mineralogy create ideal conditions for normal gilgai formation. When combined with a sloping landscape of 1 to 3°, these conditions form linear gilgai (Fig. 6).

Paleosol characteristics and productivity

There is little variability in the reconstructed soil characteristics in profiles sampled across the landscape with exception of Kisaaka 10 and Kisaaka 13, which have high CaO of 5% (Table 2) and are very close to tufa deposits mapped in Figure 1C. The lowest horizons of Paleosol 3 closest to these spring deposits have evidence for higher proportion of carbonate as syndepositional cement (Beverly et al., 2015). For example, the lowest horizon at Kisaaka 14A is much lighter in color due to the increased carbonate content (Fig. 2). Deposition of tufa ceased due to the influx of sediment, but lower horizons were likely still affected by supersaturated groundwater. These effects would disappear up section as cumulative pedogenesis continued, but may have

Table 3
Pedotransfer functions calculated from the Paleosol 3 Vertisol to reconstruct soil properties across the landscape. See Fig. 1 for location of sites.

Soil horizon	Depth cm	Total clay %	Fine clay %	FC/TC	COLE cm cm^{-1}	CEC cmolc kg^{-1}	CEC/clay	pH H_2O	BS %	ESP %	EC dS m^{-1}	Fe_d %	$CaCO_3$ %
Kisaaka 4F													
Bkss1b3	0–20	57.9	27.0	0.47	0.08	44.2	0.76	7.7	100	18	17	13	3
Bkss2b3	20–40	57.9	28.0	0.48	0.08	44.2	0.76	7.6	99	18	16	13	2
Bkss3b3	40–110	56.4	24.3	0.43	0.08	44.1	0.78	7.7	100	18	17	13	4
Bkss4b3	110–120	55.1	25.5	0.46	0.08	44	0.80	7.8	100	19	18	16	5
BCkb3	120–130	53.6	22.7	0.42	0.08	43.9	0.82	7.9	100	21	21	17	6
Kisaaka 10													
ABkb3	0–5	53.8	23.7	0.44	0.08	43.9	0.82	7.9	100	21	20	8	6
Bk1b3	5–30	56.4	27.5	0.49	0.08	44.2	0.78	7.6	99	16	13	10	3
Bk2b3	30–60	57.1	26.5	0.46	0.08	44.1	0.77	7.7	100	15	13	11	4
Bkss1b3	60–120	58.1	26.1	0.45	0.08	44.1	0.76	7.7	100	15	13	11	4
Bkss2b3	120–180	58.2	26.0	0.45	0.08	44.1	0.76	7.7	100	16	14	12	3
Bkss3b3	180–220	57.5	25.4	0.44	0.08	44.1	0.77	7.7	100	17	15	11	4
Kisaaka 13													
ABkb3	0–20	60.6	30.3	0.50	0.09	39.7	0.66	7.4	96	34	43	8	2
Bkb3	20–60	56.6	23.3	0.41	0.08	35.2	0.62	7.9	100	23	23	10	6
Bkss1b3	60–100	55.2	21.2	0.38	0.08	33.4	0.61	8.1	100	23	23	11	8
Bkss2b3	100–140	52.9	18.9	0.36	0.07	30.7	0.58	8.2	100	22	22	10	11
Bkss3b3	140–190	54.4	20.9	0.38	0.07	33	0.61	8.1	100	23	22	11	8
Bkss4b3	190–220	53.3	21.5	0.40	0.07	33.1	0.62	8	100	21	20	12	7
Kisaaka 12													
ABkb3	0–10	56.2	25.0	0.44	0.08	44	0.78	7.8	100	11	9	12	3
Bkb3	10–40	56.1	25.5	0.45	0.09	44.1	0.79	7.8	100	12	10	13	3
Bkss1b3	40–90	56.4	26.2	0.46	0.08	44.1	0.78	7.7	100	14	11	15	2
Bkss2b3	90–110	55.7	24.9	0.45	0.08	44	0.79	7.8	100	15	13	14	3
BCkb3	110–120	54.6	23.0	0.42	0.08	43.9	0.80	7.9	100	14	11	13	4

FC/TC: ratio of fine clay to total clay; COLE: coefficient of linear extensibility; CEC: cation exchange capacity; BS: base saturation; ESP: exchangeable sodium percentage; EC: electrical conductivity; Fe_d: crystalline Fe oxide.

https://doi.org/10.1016/j.yqres.2015.08.002 Published online by Cambridge University Press

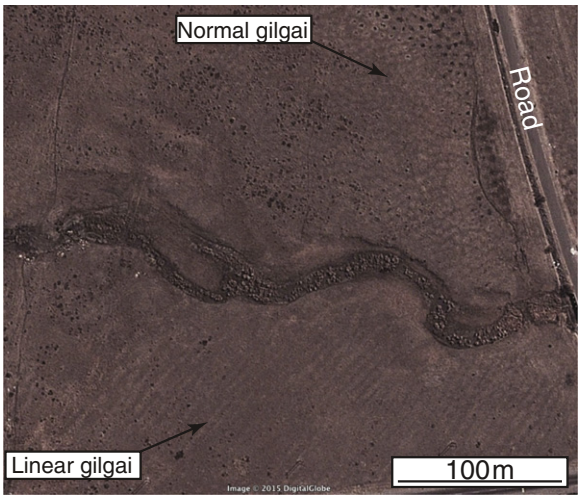

Figure 6. Modern examples of linear and normal gilgai from Rustenburg, South Africa from Google Earth (2015) (25.59°S, 27.25°E).

contributed to greater carbonate (up to 11% $CaCO_3$) in the soil matrix at Kisaaka 10 and 13, making the pH more alkaline than at other localities (Table 3).

High CEC and BS (30.7–43.9 cmolc kg^{-1} and 99–100%, respectively) indicate that the Paleosol 3 (paleo-Vertisol) would have been fertile with many plant available nutrients with an alkaline pH (7.4–8.2) that would not have affected plant size by limiting nutrient availability, which can be lost with an acidic pH (Brady and Weil, 2008). Burrows from earthworms and termites would have provided macropores favorable to root growth and microbial activity (Figs. 3C and 4L; Jongmans et al., 2001). Although the paleo-Vertisol was fertile and had a high water storage capacity due to high clay content that would support abundant vegetation, high ESP and EC indicate that this soil was affected by both high salinity and sodicity, which would have limited the types of plants able to grow on the landscape to those that were tolerant of these conditions. A saline-sodic soil is defined by a BS > 15%, an EC > 4 dS m^{-1}, and pH < 8.5 (Brady and Weil, 2008). With the exception of the upper two horizons from Kisaaka 12, all other horizons are classified as saline-sodic. Some plants are affected by as little as 2 dS m^{-1} for EC, and the saline-sodic conditions would have affected nutrient uptake and microbial activity (Brady and Weil, 2008). The saline-sodic conditions would have also caused a decrease in plant size in more tolerant species or have completely prevented the growth of species intolerant to saline-sodic conditions. Due to the trachytic–phonolitic composition of the tephra, which adds sodium-bearing primary minerals to the paleosols, the ESP and EC are likely to be maximal estimations (Nordt and Driese, 2010a). However, the amount of Na_2O in the paleosols is distinctly lower than the amount either in the Nyamsingula Tuff or the Nyamita Tuff (Table 2) indicating that it is unlikely that the high saline-sodic values in the paleosols are entirely related to differences in sodium-bearing primary minerals and likely are the result of pedogenesis.

These high-salinity conditions are common in soils in semi-arid climates (Brady and Weil, 2008). Additionally, the high Fe_d of 8 to 17% supports an interpretation of a semi-arid environment and also indicates warm and oxidizing conditions. The Fe_2O_3 concentrations are much higher in the Karungu paleosols than in those used to develop pedotransfer functions (Nordt and Driese, 2010a), which is likely due to contribution of Fe-rich tephra. However, the wt% Fe_2O_3 is between 1 to 4% higher in the paleosols than in the tephra indicating that the Fe_2O_3 content cannot be attributed solely to differences in primary iron-bearing minerals (Table 2) and instead is a pedogenic signal.

In Paleosol 3 volcaniclastic material is very limited (Fig. 4A–C) and tephra is only occasionally found filling burrows (Fig. 3D), which are likely related to burrowing following burial and termination of the soil by the Nyamita Tuff. Burrowing infill is not limited to tephra, and the meniscate backfill is often composed of the clay matrix (Fig. 4C). This indicates that the burrowing occurred for the duration of soil formation. However, as Paleosol 3 has very little volcaniclastic material in the matrix, it is unlikely that tephra accumulated throughout the life of the paleosol.

Following the deposition of the Nyamita Tuff at ~49 ka, tephra becomes much more abundant on the landscape and was likely frequently deposited during of the development of Paleosols 1 and 2. Both paleo-Inceptisols (Paleosols 1 and 2) deposited between 49 and >33 ka have significantly more tephra within burrows and the matrix (Fig. 4D). The additional tephra had physical effects on these paleosols. Although Paleosols 1 through 3 are smectitic (Fig. 5A and B) and MAP estimates suggest that the climate is similar, the addition of tephra into the depositional system seems to have limited the shrink–swell behavior of the smectite within Paleosols 1 and 2, and thus prevented the development of a Vertisol.

The lack of vertic features and less developed carbonates, which are powdery or hard masses with diffuse boundaries, would suggest that Paleosols 1 and 2 underwent shorter periods of pedogenesis (consistent with radiometric estimates of maximum formation times); however, clay coatings indicate the paleosols were forming on the landscape for intervals of time long enough to bring the paleo-Inceptisols into equilibrium with climate. Clay coatings are common in soils with high percentage of volcanic fragments (Jongmans et al., 1994), and clay coatings of up to 3% in Paleosol 2 and 5% in Paleosol 1 indicate perhaps a few thousand years of stability on the paleolandscape (Fig. 4B, C, and G–I; Soil Survey Staff, 1999; Ufnar, 2007). The age-estimate model for clay coating accumulation by Ufnar (2007) gives an estimate of ~3 ka for Paleosol 2 and ~7 ka for Paleosol 1. The illuviated clay chronofunctions developed by Ufnar (2007) were established using deeply weathered, subtropical soils from southeastern Mississippi, and therefore, a combined value of 10 ka of deposition may be an overestimation for an East African monsoonal climate. Radiometric estimates from gastropods from correlative deposits on Rusinga and Mfangano Islands (Tryon et al., 2010; Blegen et al., 2015) suggest that both Paleosols 1 and 2 were formed between 49 and >33 ka, consistent with the clay chronofunction estimate. Although Inceptisols are weakly developed soils, the degree of development of clay coatings (an Alfisol-like characteristic) provides evidence for continuous pedogenesis that would have brought the paleosols into equilibrium with the climate, supporting the MAP estimates. In addition, modern Inceptisols were included in the Marbut (1935) database used to develop the CIA-K proxy where CIA-K varied with changes in MAP (Sheldon et al., 2002).

Evidence suggests that with development of additional illuviated clay, Paleosols 1 and 2 would have eventually developed into paleo-Vertisols, as has been demonstrated in modern soils where the clay coatings reach a threshold (Stoops et al., 2010). In the Btk1b2 horizon of Paleosol 2 where the highest concentrations of clay coatings accumulated, weakly developed pedogenic slickensides are present (Table 1). Because Paleosols 1 and 2 are identified as paleo-Inceptisols, the pedotransfer functions developed for paleo-Vertisols are not applicable (Nordt and Driese, 2010a). However, the upper paleosols (1 and 2) have similar evidence of earthworms and termites that suggests that soil conditions were similar (Fig. 4A, B, E, and F; Table 1). In addition, with the exception of CaO (discussed earlier) average geochemical compositions and molecular weathering ratios indicate that Paleosols 1 and 2 likely had similar colloidal properties to Paleosol 3 that would have provided abundant nutrients (Table 2). High salinity and sodicity also likely affected Paleosols 1 and 2 due to their similarities in wt% Na_2O and Al_2O_3, which are used to estimate the ESP and EC (Table 2).

All three paleosols show evidence of redoximorphic features in which Fe and Mn have been depleted within the matrix, or concentrated

https://doi.org/10.1016/j.yqres.2015.08.002 Published online by Cambridge University Press

as coatings on peds or pores, which suggest that, at times, the soil was poorly drained. Redoximorphic features can form quickly and possibly within one wet season (Vepraskas, 1992, 2001; Vepraskas and Faulkner, 2001), but all three paleosols show evidence for drier periods as well with the precipitation of pedogenic carbonates. Paleosols 1 and 2 also have evidence for the relative timing of these features: 1) illuviated clay coatings indicative of drier climate with low water table; 2) redoximorphic FeMn coatings characteristic of a higher water table and impeded soil drainage; and 3) carbonate coatings suggestive of a return to drier conditions (Figs. 4G and 5J). The third coating of carbonate is not always present, but where it occurs, it is always in this order. This suggests that the paleosols underwent a long period of drier climate where many layers of illuviated clay coatings were deposited, followed by wetter conditions, and a return to dry conditions with the deposition of carbonate. The features in the micromorphology are likely a result of higher frequency (e.g., decadal) climate changes that occurred within an overall drier period, as indicated by the MAP estimates.

Implications for paleoclimate and paleoenvironment

Evidence from Rusinga Island and Karungu suggests that at ~94 ka the Lake Victoria region underwent a significant change in paleoclimate. Spring-fed rivers were present on the late Pleistocene landscape at Rusinga Island and Karungu, after which MAP crossed a critical recharge threshold such that the springs were choked with fluvial sediments and tufa precipitation was terminated (Beverly et al., 2015). After ~94 ka, the landscape became distinctly more fluvial with fining upward overbank floodplain deposits and paleosols. Mean annual precipitation proxies from these paleosols suggest that between 94 ka and >33 ka the Lake Victoria region experienced a significantly drier climate and environment than today.

The paleosols indicate an average paleoprecipitation range from 813 ± 108 to 963 ± 108 mm yr^{-1} using CIA-K for Paleosols 1 to 3 (Table 2). There is no evidence for a distinct change in MAP between 94 and >33 ka when these paleosols were formed, thus climate seems to have been significantly drier than modern for an extended period of time. The estimates from the Vertisol using CALMAG are lower with an average of 764 mm yr^{-1} for Paleosol 3, but CIA-K is known to overestimate paleoprecipitation in Vertisols (Nordt and Driese, 2010b). There is no evidence for diagenesis in these paleosols that would affect the paleoprecipitation estimates. There is a maximum of 2 m of modern soil above the paleosols, and all features appear to be primary with no recrystallization of pedogenic carbonates or precipitation of secondary sparry calcite that would affect the paleoprecipitation estimates using CALMAG (Fig. 4A and H). In addition, the physical evidence from the paleosols (vertic features, illuviated clay and pedogenic carbonates) and chemical evidence from pedotransfer functions (high salinity and sodicity) all suggest a highly seasonal environment and support the interpretation of an environment significantly drier than modern (~1400 mm yr^{-1}). With average CIA-K values from Paleosols 1 to 3 of 813 to 963 mm yr^{-1}, this represents a considerable reduction in precipitation relative to the present (31–42% reduction), and the first quantitative paleoprecipitation estimate for the region.

However, applying proxies developed in the United States to Eastern Africa may potentially bias the precipitation estimates because of differences in the mineralogy and chemistry of East African soils relative to those of the United States that were used in the paleosol proxy calibration datasets. Mineralogically the paleo-Vertisols of Kisaaka are similar to those of Texas used to develop the proxy: a predominantly smectitic clay mineralogy from a pre-weathered parent material (Fig. 5B; Nordt and Driese, 2010b). However, the effect of constant additions of tephra is uncertain because none of the Texas Vertisols used to develop the CALMAG proxy include volcanically influenced soils (Nordt and Driese, 2010b). The Marbut (1935) database used to develop the CIA-K proxy includes some soils with volcanically derived parent materials, but they are not abundant (Sheldon et al., 2002). Further research is needed to determine if the addition of volcaniclastic material into soils has any influence on these geochemical proxies.

Bulk geochemical analyses for each paleosol were duplicated between different localities, and in the case of Paleosol 3, samples from four localities were analyzed to capture any potential variability. The variability between individual paleosols within Paleosol units 1 and 2 is minimal and within the standard error of ± 182 for CIA-K. Paleosol 3 has more variability and at the Kisaaka 13 locality has a low MAP estimate (579 ± 108 mm yr^{-1}; CALMAG). The estimate is likely anomalously low and probably due to the proximity of the paleosol to the freshwater springs that were disappearing during the deposition of these sediments that subsequently underwent pedogenesis. The groundwater moving through these sediments would still have been supersaturated with respect to carbonate and would have resulted in additional carbonate precipitation resulting in a high average CaO of 5% in the soil matrix in comparison to other sites. MAP estimates from Paleosol 3 at other sites distal to the spring, i.e., Kisaaka 4F and 12 have CALMAG estimates of 812 ± 108 and 826 ± 108 mm yr^{-1}, respectively. Alternatively, this variability in Paleosol 3 could be attributed to problems with applying the CIA-K and CALMAG proxies to volcanically influenced East African paleosols. Regardless, the proxies still suggest that paleoprecipitation was less than modern, and they are not the only line of evidence supporting this interpretation.

The paleosol evidence is supported by the analysis of tooth enamel using the aridity index of Levin et al. (2006), which suggests a water deficit much higher than modern and a >20% reduction in MAP in the late Pleistocene (Garrett et al., 2015). Potential evapotranspiration (ET) for the Lake Victoria region greatly exceeds MAP and ranges from 2000 to 2200 mm yr^{-1} (Dagg et al., 1970). Assuming comparable values in the past, these much drier conditions during the Late Pleistocene would have resulted in a negative hydrologic budget and a significantly reduced Lake Victoria due to the sensitivity of the lake to local precipitation (Broecker et al., 1998; Milly, 1999).

In addition, Rusinga and Mfangano Islands and Karungu have the most diverse fauna of any late Pleistocene site from East Africa and abundant extinct taxa (Tryon et al., 2012; Faith, 2014; Faith et al., 2015, in press). The presence of gregarious and migratory grazers on Mfangano Island, which is too small to support viable populations of large ungulates, suggests a connection to the mainland. This requires a lake-level decline of at least 25 m (Tryon et al., 2010, 2012, 2014; Faith et al., 2011, 2012, 2014, 2015) and comparisons with existing models suggest that such a decline is only possible with a significant rainfall reduction (Broecker et al., 1998; Milly, 1999). Analyses by Faith (2013) indicate peak ungulate diversity in sub-Saharan African game reserves at ~800 mm yr^{-1} and evidence from the paleosols provide quantitative support to explain this high diversity of ungulates. Isotopic and mesowear analyses of the teeth of both ungulates and microfauna indicate an animal community dominated by a C_4 grass diet (Faith et al., 2011, 2015; Garrett et al., 2015). This C_4 grassland contrasts with the evergreen bushland, thicket, and forest habitats historically present in the region and supports the paleosol evidence for a significant reduction in precipitation. This paleosol evidence supports the hypothesis that a reduction in precipitation, coupled with expansion of grasslands and a reduced Lake Victoria facilitated the dispersal of fauna – and possibly human populations – across equatorial Africa (Cowling et al., 2008; Lorenzen et al., 2012; Faith et al., 2015, in press).

Modern analogs

The modern Vertisols of Rustenburg, South Africa have similar physical features such as grain size and gilgai topography and chemical properties such as CEC and pH. These features suggest that Rustenburg may be an appropriate modern analog. In addition, due to their low precipitation and volcanic parent material (Sinclair, 1979; Belsky, 1990), modern soils of the Serengeti (only ~150 km southeast of Karungu) are similarly saline and alkaline to the saline-sodic paleo-Vertisols and paleo-Inceptisols identified at Kisaaka. Together with MAP, soil texture

https://doi.org/10.1016/j.yqres.2015.08.002 Published online by Cambridge University Press

and the salinity and sodicity of the soils is strongly associated with vegetation type in the Serengeti (Belsky, 1990). Generally, soil catenas in the Serengeti have shallow sandy soils on ridges with short, shallowly rooted grasses and thicker, clay-rich soils (i.e. Vertisols) in the valleys with taller grasses (Bell, 1970; Belsky, 1995). Although parts of the Serengeti have enough precipitation to support trees, trees growth is limited on the Serengeti Plains due to the saline-sodic conditions (Vesey-Fitzgerald, 1973; Belsky, 1990).

The Johnson/Tothill model, a simple abiotic model for African savannas, illustrates how soil texture and precipitation greatly affect the type of vegetation (Fig. 7; Johnson and Tothill, 1985) and has been used previously to interpret paleosols in the rock record in northern Kenya (Wynn, 2000). With a MAP of ~800, the Kisaaka paleosols could support either a savanna woodland or grassland, depending on the soil texture (Johnson and Tothill, 1985; Belsky, 1990). With the higher clay contents of soils in the valleys, water penetration is poor and rivers may seasonally flood the soil, which prevents the growth of trees and shrubs (Johnson and Tothill, 1985; Belsky, 1990). Both the high salinity and sodicity and the clay-rich soil texture of Kisaaka may have contributed to the development of open grassland, which is consistent with faunal community composition and the C_4 diet of mammals from Rusinga and Mfangano Islands (Garrett et al., 2015) and Karungu (Faith et al., 2015).

Conclusions

The Kisaaka paleosols provide valuable paleoenvironmental and paleoclimatic information during a critical interval of human evolution. At ~94 ka, reduced precipitation translated to change from spring-fed rivers to soil formation. The paleosols are cumulative such that pedogenesis on the floodplain, and distal to the active channel, exceeded the rate of additions of sediments, and allowed the paleosol to come into equilibrium with the climate. The three paleosols are separated by continuous tuffs that allow for reconstruction of the landscape as a paleocatena. The oldest catena was deposited between ~94 and 49 ka and has paleo-Vertisols with abundant evidence of vertic features and exceptionally well-preserved gilgai. Pedotransfer functions suggest that paleo-Vertisols were fertile, but had saline-sodic conditions that would have affected plant growth and the types of plants growing on the landscape. The upper paleo-Inceptisols were deposited between 49 and >33 ka and the abundance of tephra had significant effects on physical characteristics by inhibiting shrinking and swelling of clays. The weathering tephra formed illuviated clay, and the degree of development of this illuviated clay suggests that these paleo-Inceptisols were in equilibrium with the climate and provides support for the paleoprecipitation estimates.

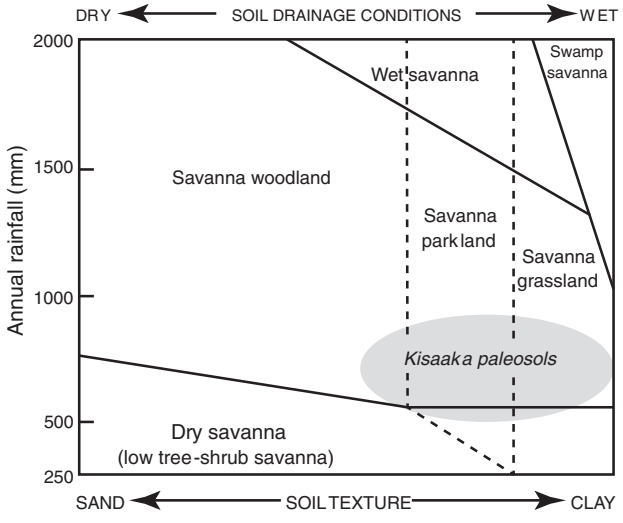

Figure 7. The Kisaaka paleosols are plotted on the Johnson/Tothill model of tropical savannas, which uses soil texture and annual precipitation.
Modified from Johnson and Tothill, 1985.

The paleosol MAP estimates suggest a similar paleoclimate between ~94 and 49 ka with MAP ranges from 764 ± 182 mm yr^{-1} for Vertisols (CALMAG) and 813 to 963 ± 108 mm yr^{-1} for all other paleosols (CIA-K) with no significant changes in paleoprecipitation between paleosols. This reduction in precipitation would have resulted in a significant reduction in the size of Lake Victoria, and represent the first paleoprecipitation estimates for the region during the late Pleistocene. The drop in precipitation and the saline-sodic conditions of these paleosols supports the interpretation of the expansion of semi-arid C_4 grasslands made based on fossil and stable C and O isotope analyses. Together, all lines of evidence suggest that the Serengeti may represent a modern analog for the late Pleistocene paleolandscape at Kisaaka.

Supplementary data to this article can be found online at http://dx.doi.org/10.1016/j.yqres.2015.08.002.

Acknowledgments

Fieldwork at Rusinga Island and Karungu was conducted under research permits NCST/5/002/R/605 issued to EJB, NCST/RCD/12B/01/07 issued to DJP, NCST/RCD/12B/012/31 issued to JTF, NCST/5/002/R605 issued to SGD, and NCST/5/002/R/576 issued to CAT. We greatly appreciate the support of the National Museum of Kenya (NMK), especially Drs. E. Mbua and F. Manthi, and funding from the National Geographic Society Committee for Research and Exploration (9284-13 and 8762-10), the National Science Foundation (BCS-1013199 and BCS-1013108), the Leakey Foundation, the Geological Society of America, the Society for Sedimentary Geology (SEPM), the University of Queensland, Baylor University, the Baylor University Department of Geology Dixon Fund, New York University, Harvard University, and the American School for Prehistoric Research. We also greatly appreciate the assistance of S. Longoria of the NMK and Z. Ogutu in the field. Finally, we thank Drs. Nordt, Dworkin, and Ferraro of Baylor University for their helpful comments and discussion.

References

Ambrose, S.H., Lorenz, K.G., 1990. Social and ecological models for the Middle Stone Age in southern Africa. In: Mellars, P. (Ed.), The Emergence of Modern Humans: And Archaeological Perspective. Edinburgh University Press, Edinburgh, pp. 3–33.
Angelucci, D.E., 2010. The recognition and description of knapped lithic artifacts in thin section. Geoarchaeology 25, 220–232.
Beckmann, G.G., Hubble, G.D., Thompson, C.H., 1970. Gilgai forms, distribution and soil relationships in North-Eastern Australia. Proceedings of the Symposium on Soils and Earth Structures in Arid Climates; Adelaide, 21–22, May 1970. The Institution of Engineers, Australia, pp. 116–121 (Adelaide).
Beckmann, G.G., Thompson, C.H., Hubble, G.D., 1973. Linear gilgai. Australian Geographer 12, 363–366.
Bell, R.H.V., 1970. The use of the herb layer by grazing ungulates in the Serengeti. In: Watson, A. (Ed.), Animal Populations in Relation to their Food Resources. Blackwell, Oxford, pp. 111–124.
Belsky, A.J., 1990. Tree/grass ratios in East African savannas: a comparison of existing models. Journal of Biogeography 17, 483–489.
Belsky, J.A., 1995. Spatial and temporal landscape patterns in arid and semi-arid African savannas. In: Hansson, L., Fahrig, L., Merriam, G. (Eds.), Mosaic Landscapes and Ecological Processes. Chapman & Hall, London, pp. 31–56.
Berke, M.A., Johnson, T.C., Werne, J.P., Grice, K., Schouten, S., Sinninghe Damsté, J.S., 2012. Molecular records of climate variability and vegetation response since the Late Pleistocene in the Lake Victoria basin, East Africa. Quaternary Science Reviews 55, 59–74.
Beverly, E.J., Driese, S.G., Peppe, D.J., Johnson, C.R., Michel, L.A., Faith, J.T., Tryon, C.A., Sharp, W.D., 2015. Recurrent spring-fed rivers in a Middle to Late Pleistocene semi-arid grassland: implications for environments of early humans in the Lake Victoria Basin, Kenya. Sedimentology http://dx.doi.org/10.1111/sed.12199.
Birkeland, P.W., 1999. Topography–soil relations with time in different climatic settings. Soils and Geomorphology. Oxford University Press, New York, pp. 230–267.
Bishop, W.W., Trendall, A.F., 1967. Erosion-surfaces, tectonics and volcanic activity in Uganda. Quarterly Journal of the Geological Society 122, 385–420.
Blegen, N., Tryon, C.A., Faith, J.T., Peppe, D.J., Beverly, E.J., Li, B., Jacobs, Z., 2015. Distal tephras of the eastern Lake Victoria Basin, equatorial East Africa: correlations, chronology, and a context for early modern humans. Quaternary Science Reviews 122, 89–111.
Blome, M.W., Cohen, A.S., Tryon, C.A., Brooks, A.S., Russell, J., 2012. The environmental context for the origins of modern human diversity: a synthesis of regional variability

in African climate 150,000–30,000 years ago. Journal of Human Evolution 62, 563–592.
Bootsma, H.A., Hecky, R.E., 2003. A comparative introduction to the biology and limnology of the African Great Lakes. Journal of Great Lakes Research 29, 3–18.
Brady, N.C., Weil, R.R., 2008. The Nature and Properties of Soils. 14th ed. Pearson Prentice Hall, New Jersey.
Brimhall, G.H., Dietrich, W.E., 1987. Constitutive mass balance relations between chemical composition, volume, density, porosity, and strain in metasomatic hydrochemical systems: results on weathering and pedogenesis. Geochimica et Cosmochimica Acta 51, 567–587.
Broecker, W.S., Peteet, D., Hajdas, I., Lin, J., Clark, E., 1998. Antiphasing between rainfall in Africa's Rift Valley and North America's Great Basin. Quaternary Research 50, 12–20.
Brown, F.H., McDougall, I., Fleagle, J.G., 2012. Correlation of the KHS Tuff of the Kibish Formation to volcanic ash layers at other sites, and the age of early *Homo sapiens* (Omo I and Omo II). Journal of Human Evolution 63, 577–585.
Burt, R. (Ed.), 2011. Soil Survey Laboratory Information Manual: Soil Survey Investigations Report No. 45. USDA NRCS, Nebraska.
Caudill, M.R., Driese, S.G., Mora, C.I., 1996. Preservation of a paleo-Vertisol and an estimate of Late Mississippian paleoprecipitation. Journal of Sedimentary Research 66, 58–70.
Chadwick, O.A., Brimhall, G.H., Hendricks, D.M., 1990. From a black to a gray box — a mass balance interpretation of pedogenesis. Geomorphology 3, 369–390.
Cowling, S.A., Cox, P.M., Jones, C.D., Maslin, M.A., Peros, M., Spall, S.A., 2008. Simulated glacial and interglacial vegetation across Africa: implications for species phylogenies and trans-African migration of plants and animals. Global Change Biology 14, 827–840.
Crul, R.C.M., 1995. Limnology and hydrology of Lake Victoria. Comprehensive and Comparative Study of Great Lakes. UNESCO, p. 79.
Dagg, M., Woodhead, T., Rijks, D.A., 1970. Evaporation in East Africa. Bulletin of the International Association of Scientific Hydrology 15, 61–67.
Doornkamp, J.C., Temple, P.H., 1966. Surface, drainage and tectonic instability in part of southern Uganda. The Geographical Journal 132, 238–252.
Driese, S.G., Mora, C.I., Stiles, C.A., Joeckel, R.M., Nordt, L.C., 2000. Mass-balance reconstruction of a modern Vertisol: implications for interpreting the geochemistry and burial alteration of paleo-Vertisols. Geoderma 95, 179–204.
Driese, S.G., Jacobs, J.R., Nordt, L.C., 2003. Comparison of modern and ancient Vertisols developed on limestone in terms of their geochemistry and parent material. Sedimentary Geology 157, 49–69.
Ebinger, C.J., 1989. Tectonic development of the western branch of the East African rift system. GSA Bulletin 101, 885–903.
Eriksson, A., Betti, L., Friend, A.D., Lycett, S.J., Singarayer, J.S., von Cramon-Taubadel, N., Valdes, P.J., Balloux, F., Manica, A., 2012. Late Pleistocene climate change and the global expansion of anatomically modern humans. Proceedings of the National Academy of Sciences of the United States of America 109, 16089–16094.
Faith, J.T., 2013. Ungulate diversity and precipitation history since the Last Glacial Maximum in the Western Cape, South Africa. Quaternary Science Reviews 68, 191–199.
Faith, J.T., 2014. Late Pleistocene and Holocene mammal extinctions on continental Africa. Earth-Science Reviews 128, 105–121.
Faith, J.T., Choiniere, J.N., Tryon, C.A., Peppe, D.J., Fox, D.L., 2011. Taxonomic status and paleoecology of *Rusingoryx atopocranion* (Mammalia, Artiodactyla), an extinct Pleistocene bovid from Rusinga Island, Kenya. Quaternary Research 75, 697–707.
Faith, J.T., Potts, R., Plummer, T.W., Bishop, L.C., Marean, C.W., Tryon, C.A., 2012. New perspectives on middle Pleistocene change in the large mammal faunas of East Africa: *Damaliscus hypsodon* sp. nov. (Mammalia, Artiodactyla) from Lainyamok, Kenya. Palaeogeography Palaeoclimatology Palaeoecology 361–362, 84–93.
Faith, J.T., Tryon, C.A., Peppe, D.J., Beverly, E.J., Blegen, N., 2014. Biogeographic and evolutionary implications of an extinct Late Pleistocene impala from the Lake Victoria Basin, Kenya. Journal of Mammalian Evolution 21, 213–222.
Faith, J.T., Tryon, C.A., Peppe, D.J., Beverly, E.J., Blegen, N., Blumenthal, S., Chritz, K., Driese, S.G., Patterson, D., 2015. Paleoenvironmental context of the Middle Stone Age record from Karungu, Lake Victoria Basin, Kenya, and its implications for human and faunal dispersal in East Africa. Journal of Human Evolution 83, 28–45.
Faith, J.T., Tryon, C.A., Peppe, D.J., 2015. Environmental change, ungulate biogeography, and their implications for early human dispersals in equatorial East Africa. In: Jones, S.C., Stewart, B.A. (Eds.), Africa from MIS 6-2: Population Dynamics and Paleoenvironments. Springer (in press).
Fey, M., Hughes, J., Lambrechts, J., Dohse, T., 2010. Vertic soils. Soils of South Africa. Cambridge University Press, Cape Town, South Africa, pp. 35–45.
Fillinger, U., Sonye, G., Killeen, G.F., Knols, B.G.J., Becker, N., 2004. The practical importance of permanent and semipermanent habitats for controlling aquatic stages of *Anopheles gambiae* sensu lato mosquitoes: operational observations from a rural town in western Kenya. Tropical Medicine & International Health 9, 1274–1289.
Fitzpatrick, E.A., 1993. Soil Microscopy and Micromorphology. John Wiley & Sons, New York.
Garrett, N.D., Fox, D.L., McNulty, K.P., Tryon, C.A., Faith, J.T., Peppe, D.J., Plantinga, A. Van, 2015. Stable isotope paleoecology of Late Pleistocene Middle Stone Age humans from the equatorial East Africa, Lake Victoria basin, Kenya. Journal of Human Evolution 82, 1–14.
Google Earth, 2015. Rustenburg Linear Gilgai, 25°35′24.30″S, 27°15′11.49″E, elev 3636 ft, July 14, 2011 (Accessed January 20, 2015).
Hallsworth, E.G., Beckman, G.G., 1969. Gilgai in the Quaternary. Soil Science 107, 409–420.
Hallsworth, E.G., Robertson, G.K., Gibbons, F.R., 1955. Studies in pedogenesis in New South Wales. Journal of Soil Science 6, 1–31.
Johnson, R.W., Tothill, J.C., 1985. Definitions and broad geographic outline of savanna lands. In: Tothill, J.C., Mott, J.J. (Eds.), Ecology and management of the world's savannas. Australian Academy of Science, Canberra, pp. 1–13.
Johnson, T.C., Scholz, C.A., Talbot, M.R., Kelts, K., Ricketts, R.D., Ngobi, G., Beuning, K.R., Ssemmanda, I., McGill, J.W., 1996. Late Pleistocene dessication of Lake Victoria and rapid evolution of cichlid fishes. Science 273, 1091–1093.
Jongmans, A.G., van Oort, F., Buurman, P., Jaunet, A.M., van Doesburg, J.D.J., 1994. Morphology, Chemistry, and Mineralogy of Isotropic Aluminosilicate Coatings in a Guadeloupe Andisol. Soil Science Society of America Journal 58, 501–507.
Jongmans, A.G., Pulleman, M.M., Marinissen, J.C.Y., 2001. Soil structure and earthworm activity in a marine silt loam under pasture versus arable land. Biology and Fertility of Soils 33, 279–285.
Jungerius, P.D., Van Den Ancker, J.A.M., Mucher, H.J., 1999. The contribution of termites to the microgranular structure of soils on the Uasin Gishu Plateau, Kenya. Catena 34, 349–363.
Kendall, R.L., 1969. An ecological history of the Lake Victoria Basin. Ecological Monographs 39, 121–176.
Kent, P.E., 1944. The age and tectonic relationships of East African Volcanic Rocks. Geological Magazine 81, 15–27.
Kraus, M.J., 1999. Paleosols in clastic sedimentary rocks: their geologic applications. Earth-Science Reviews 47, 41–70.
Levin, N.E., Cerling, T.E., Passey, B.H., Harris, J.M., Ehleringer, J.R., 2006. A stable isotope aridity index for terrestrial environments. Proceedings of the National Academy of Sciences 103, 11201–11205.
Lorenzen, E.D., Heller, R., Siegismund, H.R., 2012. Comparative phylogeography of African savannah ungulates. Molecular Ecology 21, 3656–3670.
Marbut, C.F., 1935. Atlas of American. III. Soils of the United States. Government Printing Office, Washington, D.C.
McBrearty, S., Brooks, A.S., 2000. The revolution that wasn't: a new interpretation of the origin of modern human behavior. Journal of Human Evolution 39, 453–563.
McDougall, I., Brown, F.H., Fleagle, J.G., 2005. Stratigraphic placement and age of modern humans from Kibish, Ethiopia. Nature 433, 733–736.
Milly, P.C.D., 1999. Comment on "Antiphasing between rainfall in Africa's Rift Valley and North America's Great Basin." Quaternary Research 51, 104–107.
Milne, G., 1936. Natural erosion as a factor in soil profile development. Nature 138, 548–549.
Moore, D.M., Reynolds, R.C., 1997. X-Ray Diffraction and the Identification and Analysis of Clay Minerals. Oxford University Press, New York, p. 378.
Mora, C.I., Driese, S.G., 1999. Palaeoclimatic significance and stable carbon isotopes of Palaeozoic red bed paleosols, Appalachian Basin, USA and Canada. In: Thiry, M., Simon-Coinçon, R. (Eds.), Palaeoweathering, Palaeosurfaces and Related Continental Deposits. International Association of Sedimentologists Special Publication No. 27, pp. 61–84.
Nordt, L.C., Driese, S.G., 2009. Hydropedological assessment of a vertisol climosequence on the Gulf Coast Prairie Land Resource Area of Texas. Hydrology and Earth System Sciences 13, 2039–2053.
Nordt, L.C., Driese, S.G., 2010a. A modern soil characterization approach to reconstructing physical and chemical properties of paleo-Vertisols. American Journal of Science 310, 37–64.
Nordt, L.C., Driese, S.G., 2010b. New weathering index improves paleorainfall estimates from Vertisols. Geology 38, 407–410.
Owen, W.E., 1937. Draft of tentative preliminary report on the July 1937 investigations at Ng'ira Karungu. Unpublished manuscript housed in the archives of the Natural History Museum, London.
Owen, W.E., 1938. The Kombewa Culture, Kenya Colony. Man 38, 203–205.
Owen, W.E., 1939. An amateur field collector in Kavirondo, part II. Journal of the Royal African Society 38, 220–226.
Pickford, M.H., 1984. An aberrant new bovid (Mammalia) in subrecent deposits from Rusinga island, Kenya. Proceedings of the Koninklijke Nederlandse Akademie Van Wetenschappen Series B: Palaeontology, Geology, Physics, Chemistry, Anthropology 87, 441–452.
Retallack, G.J., 2001. Soils of the Past: An Introduction to Paleopedology. 2nd ed. Blackwell Science Ltd, Oxford.
Rito, T., Richards, M.B., Fernandes, V., Alshamali, F., Cerny, V., Pereira, L., Soares, P., 2013. The first modern human dispersals across Africa. PLoS One 8, 1–16.
Scholz, C.A., Johnson, T.C., Cohen, A.S., King, J.W., Peck, J.A., Overpeck, J.T., Talbot, M.R., Brown, E.T., Kalindekafe, L., Amoako, P.Y., Lyons, R.P., Shanahan, T.M., Castaneda, I.S., Heil, C.W., Forman, S.L., McHargue, L.R., Beuning, K.R., Gomez, J., Pierson, J., 2007. East African megadroughts between 135 and 75 thousand years ago and bearing on early-modern human origins. Proceedings of the National Academy of Sciences of the United States of America 104, 16416–16421.
Sheldon, N.D., Tabor, N.J., 2009. Quantitative paleoenvironmental and paleoclimatic reconstruction using paleosols. Earth-Science Reviews 95, 1–52.
Sheldon, N.D., Retallack, G.J., Tanaka, S., 2002. Geochemical climofunctions from North America soils and applications to paleosols across the Eocene–Oligocene boundary in Oregon. Journal of Geology 110, 687–696.
Sinclair, A.R.E., 1979. The Serengeti Environment. In: Sinclair, A.R.E., Norton-Griffiths, M. (Eds.), The University of Chicago Press, Chicago, pp. 31–45.
Soares, P., Alshamali, F., Pereira, J.B., Fernandes, V., Silva, N.M., Afonso, C., Costa, M.D., Musilova, E., Macaulay, V., Richards, M.B., Cerny, V., Pereira, L., 2012. The expansion of mtDNA Haplogroup L3 within and out of Africa. Molecular Biology and Evolution 29, 915–927.
Soil Survey Staff, 1999. Soil Taxonomy: A Basic System of Soil Classification for Making and Interpreting Soil Surveys. 2nd ed. USDA NRCS, Washington D.C.
Song, Y., Semazzi, F.H.M., Xie, L., Ogallo, L.J., 2004. A coupled regional climate model for the Lake Victoria Basin of East Africa. International Journal of Climatology 24, 57–75.
Stager, J.C., Johnson, T.C., 2008. The late Pleistocene desiccation of Lake Victoria and the origin of its endemic biota. Hydrobiologia 596, 5–16.

https://doi.org/10.1016/j.yqres.2015.08.002 Published online by Cambridge University Press

Stager, J.C., Mayewski, L., Meeker, L.D., 2002. Cooling cycles, Heinrich event 1, and the desiccation of Lake Victoria. Palaeogeography Palaeoclimatology Palaeoecology 183, 169–178.
Stager, J.C., Ryves, D.B., Chase, B.M., Pausata, F.S.R., 2011. Catastrophic drought in the Afro-Asian monsoon region during Heinrich Event 1. Science 331, 1299–1302.
Stoops, G., 2003. Guidelines for Analysis and Description of Soil and Regolith Thin Sections. Soil Science Society of America, Inc., Madison, Wisconsin.
Stoops, G., Marcelino, V., Mees, F. (Eds.), 2010. Interpretation of Micromorphological Features of Soils and Regoliths, 1st ed. Elsevier, Netherlands.
Tabor, N.J., Myers, T.S., 2015. Paleosols as indicators of paleoenvironment and paleoclimate. Annual Review of Earth and Planetary Sciences 43, 11.1–11.29.
Talbot, M.R., Laerdal, T., 2000. The late Pleistocene–Holocene palaeolimnology of Lake Victoria, East Africa, based upon elemental and isotopic analyses of sedimentary organic matter. Journal of Paleolimnology 23, 141–164.
Talbot, M.R., Williams, M.A.J., 2009. Cenozoic evolution of the Nile Basin. In: Dumont, H.J. (Ed.), The Nile: Origin, Environments, Limnology and Human Use. Springer Science + Business Media B.V, pp. 37–60.
Tryon, C.A., Faith, J.T., 2013. Variability in Middle Stone Age of Eastern Africa. Current Anthropology 54, S234–S254.
Tryon, C.A., Faith, J.T., Peppe, D.J., Fox, D.L., McNulty, K.P., Jenkins, K., Dunsworth, H., Harcourt-Smith, W., 2010. The Pleistocene archaeology and environments of the Wasiriya Beds, Rusinga Island, Kenya. Journal of Human Evolution 59, 657–671.
Tryon, C.A., Peppe, D.J., Faith, J.T., Van Plantinga, A., Nightingale, S., Ogondo, J., Fox, D.L., 2012. Late Pleistocene artefacts and fauna from Rusinga and Mfangano islands, Lake Victoria, Kenya, Azania. Archaeological Research in Africa 47, 14–38.
Tryon, C.A., Faith, J.T., Peppe, D.J., Keegan, W.F., Keegan, K.N., Jenkins, K.H., Nightingale, S., Patterson, D., Van Plantinga, A., Driese, S., Johnson, C.R., Beverly, E.J., 2014. Sites on the landscape: paleoenvironmental context of late Pleistocene archaeological sites from the Lake Victoria basin, equatorial East Africa. Quaternary International 331, 20–30.
Ufnar, D., 2007. Clay coatings from a modern soil chronosequence: a tool for estimating the relative age of well-drained paleosols. Geoderma 141, 181–200.
Van Plantinga, A.A., 2011. Geology of the Late Pleistocene Artifact-bearing WAsiriya Beds at the Nyamita Locality, Rusinga Island, Kenya (M.S. Thesis) Baylor Unviersity.
Vepraskas, M.J., 1992. Redoximorphic features for identifying aquic conditions. North Carolina Agricultural Research Service Technical Bulletin 301 (33 pp.).
Vepraskas, M.J., 2001. Morphological features of seasonally reduced soils. In: Richardson, J.L., Vepraskas, M.J. (Eds.), Wetland Soils: Genesis, Hydrology, Landscapes, and Classification. Lewis Publishers, New York, pp. 163–182.
Vepraskas, M.J., Faulkner, S.P., 2001. Redox chemistry of hydric soils. In: Richardson, J.L., Vepraskas, M.J. (Eds.), Wetland Soils: Genesis, Hydrology, Landscapes, and Classification. Lewis Publishers, New York, pp. 85–105.
Verster, E., de Villiers, J.M., Scheepers, J.C., 1973. Gilgai in the Rustenburg area. Agrochemophysica 4, 57–62.
Vesey-Fitzgerald, D., 1973. East African Grasslands. East African Publishing House, Nairobi.
Wynn, J.G., 2000. Paleosols, stable carbon isotopes, and paleoenvironmental interpretation of Kanapoi, Northern Kenya. Journal of Human Evolution 39, 411–432.

https://doi.org/10.1016/j.yqres.2015.08.002 Published online by Cambridge University Press